**Naval Research Laboratory**
Washington, DC 20375-5320

NRL/MR/6790--03-8656

# In-situ Measurements of Temperature Profiles and Plume Formation at the Surfaces of Samples Irradiated by a Picosecond Laser Pulse Train

J. GRUN
R. FISCHER

*Beam Physics Branch*
*Plasma Physics Division*

C. K. MANKA

*Research Support Instruments*
*Lanham, MD*

R. F. WENZEL

*Directed Energy Effects Branch*
*Material Science and Technology Division*

R. COZZENS

*Materials Chemistry Branch*
*Chemistry Division*

M. SHINN

*Jefferson Laboratory*
*Newport News, VA*

July 3, 2003

# REPORT DOCUMENTATION PAGE

*Form Approved*
*OMB No. 0704-0188*



| 1. REPORT DATE *(DD-MM-YYYY)* | 2. REPORT TYPE | 3. DATES COVERED *(From - To)* |
|---|---|---|
| July 3, 2003 | | |

**4. TITLE AND SUBTITLE**

In-situ Measurements of Temperature Profiles and Plume Formation at the Surfaces of Samples Irradiated by a Picosecond Laser Pulse Train

**5a. CONTRACT NUMBER**

**5b. GRANT NUMBER**

**5c. PROGRAM ELEMENT NUMBER**
0602890D8Z

**6. AUTHOR(S)**

J. Grun, R. Fischer, C.K. Manka,* R.F. Wenzel, R. Cozzens, and M. Shinn†

**5d. PROJECT NUMBER**

**5e. TASK NUMBER**

**5f. WORK UNIT NUMBER**

**7. PERFORMING ORGANIZATION NAME(S) AND ADDRESS(ES)**

Naval Research Laboratory
4555 Overlook Avenue, SW
Washington, DC 20375-5320

**8. PERFORMING ORGANIZATION REPORT NUMBER**

NRL/MR/6790--03-8656

**9. SPONSORING / MONITORING AGENCY NAME(S) AND ADDRESS(ES)**

High Energy Laser Joint Technology Office (HEL-JTO)
901 University Boulevard, SE
Albuquerque, NM 87106

**10. SPONSOR / MONITOR'S ACRONYM(S)**

**11. SPONSOR / MONITOR'S REPORT NUMBER(S)**

**12. DISTRIBUTION / AVAILABILITY STATEMENT**

Approved for public release; distribution is unlimited.

**13. SUPPLEMENTARY NOTES**

*Research Support Instruments, 4325 Forbes Boulevard, Suite B, Lanham, MD 20706-4854
†Jefferson Laboratory, 12000 Jefferson Avenue, Newport News, VA 23606

**14. ABSTRACT**

One-inch diameter samples of various materials, such as stainless steel, painted and unpainted aluminum, fused silica, and fiberglass composites, were irradiated by a train of picosecond-duration pulses from a free-electron laser at irradiances of 0.5 to 10 kW/cm$^2$. These experiments were the first to examine the lethality of a train of picosecond-duration laser pulses in an irradiance regime relevant to high energy laser lethality, i.e., utilizing laser intensities that have a change of propagating a significant distance in the atmosphere. In situ diagnostics were used to measure space and time resolved temperature profiles on the laser-irradiated and back sides of the samples. Also, plumes emanating from the laser-irradiated side of the samples were recorded. Heating and cooling of the samples, melting, boiling, hole burning, flow of liquid matter, and breakup of composites were measured. Results of these experiments and a comparison to post-shot analysis of the samples are presented.



**15. SUBJECT TERMS**

Lethality; Laser; Picosecond; Free-electron; Plume; Temperature; Q*

| 16. SECURITY CLASSIFICATION OF: | | | 17. LIMITATION OF ABSTRACT | 18. NUMBER OF PAGES | 19a. NAME OF RESPONSIBLE PERSON |
|---|---|---|---|---|---|
| a. REPORT | b. ABSTRACT | c. THIS PAGE | | | J. Grun |
| Unclassified | Unclassified | Unclassified | UL | 54 | 19b. TELEPHONE NUMBER *(include area code)* (202) 767-9117 |

**Standard Form 298 (Rev. 8-98)**
**Prescribed by ANSI Std. Z39.18**

TABLE OF CONTENTS

## Nomenclature

Q*: Laser energy in kilo Joules required for removing one gram of material.

$\Delta\varphi$: Phase change in radians undergone by a diagnostic laser passing through a gas.

v: Index of refraction of neutral gas at density $n_0$.

$\lambda$: Laser wavelength.

L: The distance through which a diagnostic laser beam propagates.

e: Electron charge.

m: Electron mass.

c: Speed of light in vacuum.

$n_{neutral}$: Density of the neutral atoms.

$n_{electron}$: Density of free, i.e. unbound, electrons.

# IN-SITU MEASUREMENTS OF TEMPERATURES ON THE SURFACE OF SAMPLES IRRADIATED BY A PICOSECOND LASER PULSE TRAIN

## The FEL HEL Experiment

During June 20-30 and September 17-28, 2001 two campaigns examined the vulnerability of various materials to irradiation by a train of picosecond-duration pulses from a free-electron-laser at irradiances of 0.5 to 10kW/cm$^2$. These experiments were the first to examine the material damage potential of a train of picosecond-duration laser pulses in an irradiance regime relevant to High Energy Laser Lethality (HEL), i.e. utilizing laser intensities that have a chance of propagating a significant distance in the atmosphere without much loss of energy. The laser used was the Jefferson Laboratory's free electron laser (FEL) operating at a wavelength of 3.1 micron; pulse duration of 1 pico-second; average powers of 300 Watts, 600 Watts, and 1000 Watts; with pulse-repetition-rates of 18.71 MHz, 37.42 MHz, and 74.85 MHz. Most irradiation were done with the sample in an uncharacterized airflow of about Mach 0.1 (90 mph) from a nozzle directed upward, about 30 degrees from vertical, across its front face. Five hundred and ninety four samples were tested, among them samples of stainless steel, painted and unpainted aluminum, and a variety of materials used in radomes –such as glass-cloth composites, Pyroceram, and fused silica. A detailed shot matrix is given in Jefferson Laboratory's report on these experiments[1] and at the end of this paper. The reader is advised to read JLAB's report together with ours to get a complete picture of these experiments and their results.

[1] Michelle D. Shinn and George R. Neil, *Femto-second, Pulsed, and CW Laser Effects Testing* (2003). Manuscript approved April 8, 2003.

Diagnostics designed to measure the efficiency with which the FEL damages the different tested materials, parameters of the laser pulse, and certain details of the laser-material interaction were fielded by JLAB and NRL. The diagnostics fielded by JLAB include:

- Monitor of the input laser power (Molectron PM30 power meter)
- Monitor of the reflected laser power (Molectron PM-5K power meter)
- Photograph of the time-integrated beam profile (Spiricon Pyrocam I)
- Video of the front of the target during laser irradiance
- Diode placed in back of the target to measure time to target burn-through (Thorlabs DET2)

Q* measurements were obtained using two methods, penetration time and mass removal. On metallic samples which were penetrated by the laser, Q* was inferred from the equation $Q^* = I\ t/\rho\ d$, where I is the irradiance in KWatts/cm$^2$, d and $\rho$ are respectively the sample thickness and density, and t is the time to penetrate the sample. Penetration time was measured with a diode viewing laser light that penetrated the sample and reflected from a graphite slab placed behind the sample to serve as a laser beam dump. For samples which were not penetrated, mostly the non-metals, the sample was weighed before and after irradiation and Q*inferred from Q*=Laser Kilo Joules /weight loss in grams.

Our, i.e. NRL's, task during these experiments was to field time and space resolved *in situ* diagnostics that would measure certain details of the laser-target interaction. Detailed measurements of the interaction inject additional science into the experiments,

provide data that could be used to validate predictive laser-matter interaction codes, and provide increased confidence (or lack thereof) in the validity of Q* measurements and their extrapolation to full-scale weapons scenarios. We chose to field two four-color video cameras, a time-resolved spectrometer, and a time-resolved interferometer. All together, the four-color cameras were used on 300 tests producing 47,000 images, the spectrometer was used on 250 tests producing 27,000 spectra, and the interferometer was used on about 200 tests.

The subject of this report is a description of the in-situ diagnostics, their calibration, and the results they produced. The report describes and discusses typical results seen on each target type. A complete list of acquired and good data is given at the end of the report.

In the discussion that follows, the reader will note that particular tests are referred to as "Suite #-##", for example "Suite 1-2". The meaning of this designation is this: In these experiments six samples ("targets") were mounted at one time on a motorized holder. On a signal from the FEL control room each target was rotated into the location where it could be irradiated by the FEL laser beam. Once a particular target was in place the FEL was turned on and the test commenced. Thus, in the designation "Suite #-##", Suite # refers to a group of six targets designated by the number #, and ## refers to the ##'s sample in the suite that was exposed to the laser beam. The reader may also come across the terminology "Suite # run ##", or Suite # slot ##". All these designations refer to the same thing.

## *In Situ* Diagnostics

Three types of real-time, *in situ* diagnostics were deployed; two four-color video cameras – one observing the front (i.e. laser-illuminated) and one the back (side away from laser beam) of the target, a time-resolved spectrometer observing the front of the target, and a space and time-resolved interferometer that observed the target edge on. The diagnostics are capable of measuring the following phenomena:

- Four-color video cameras
    - Emission temperature of the laser-heated spot on the target front as a function of space and time.
    - Emission temperature of the target rear as a function of space and time. Time to burn-through is easily observed and can be correlated with temperature profiles on the front, laser-illuminated side.
    - Heat conduction in the lateral and axial directions.
    - Disassembly of composite materials, mass flow at the target front or rear, melting, boiling, and vaporization processes.

- Time-resolved spectrometer
    - Spatially-averaged, time-resolved emission temperatures from the front of the sample.
    - Line spectra of the laser beam harmonics and from the target material, if hot enough. This spectrometer is also needed to verify the black/grey

body assumptions used by the deconvolution algorithms of the four-color imager.

- Space and time-resolved interferometer
    - Absorption conditions in front of the target.
    - Density of plumes, if any, and plume dynamics. Ejected material or droplets.

The relative locations of the diagnostics are shown in Figure 1.

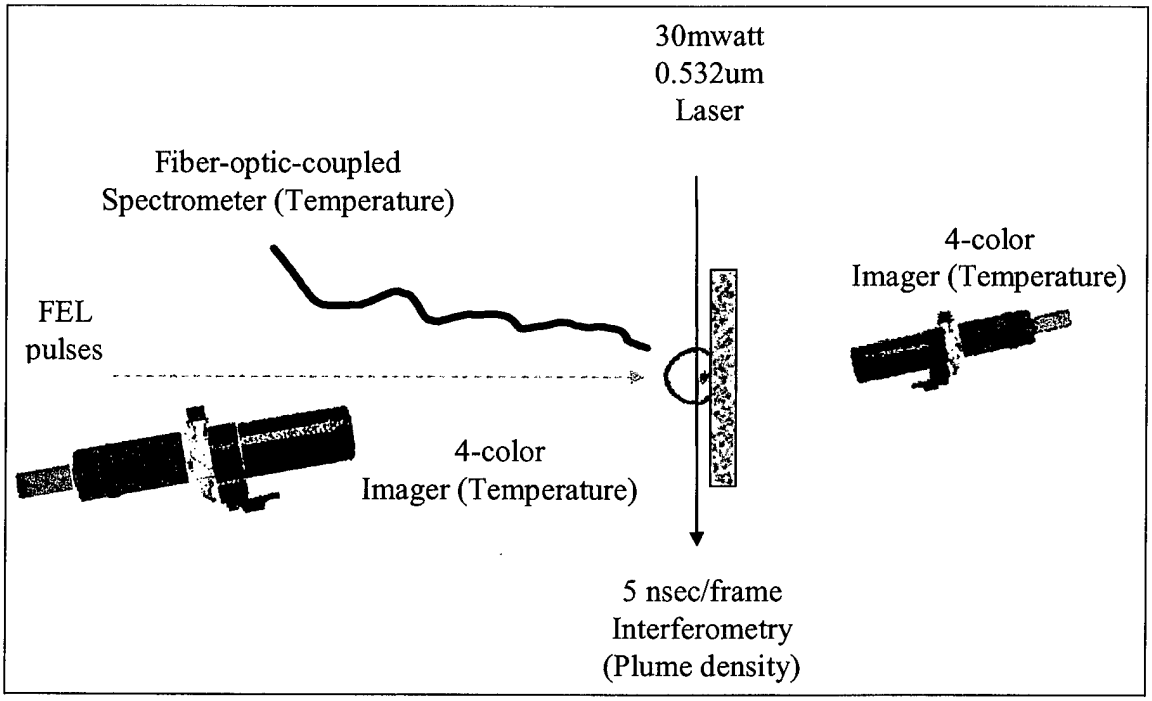


**Figure 1: Setup of NRL diagnostics in the experiment. The front four color camera is placed at 18 degrees to the target and 78cm away. The rear camera is placed at 15 degrees to the target and 31 cm away. A fiber-optic-coupled spectrometer measures emitted light from a 3mm diameter spot on the front of the heated target. The interferometer images an approximately 1-inch-square region in front of the target with a 5nsec temporal resolution.**

## *Four-Color Camera*

Each of the two four-color video cameras uses a photographic lens to collect and collimate light emitted by the target. A triple-dichroic/single-mirror module is placed in the path of the collimated light[2] to split the parallel light beam into four separate components, each containing a different part of the incident spectrum. The spectral content of each beam is further refined by placing a narrow band-pass filter in its path. The four filters in our case were centered at 700, 750, 800, and 850 nanometers with bandwidths of 20, 40, 40, and 40 nanometers respectively. After filtering, each beam passes through a common imaging lens, forming four simultaneously-acquired spatially-identical, but spectrally-different images of the light emitting region on a single 1034 by 779 pixel CCD camera chip, each image occupying one quadrant of the CCD detector area. The four images are continuously read out of the CCD and stored on a computer disk at a rate of 7-10 frames/second. The software running the camera has been customized for this FEL experiment to achieve the stated acquisition rate, allow immediate review of data after a test, provide for semiautomatic analysis of data, and for production of movie sequences.

The use of four spectrally-filtered images is important for accurate determination of temperature. A temperature can be estimated, and often is, from one or two-color pyrometers. To infer a temperature with these diagnostics, however, one must assume that a material's emissivity[3] is known *a priory* and that its value does not vary with

[2] Placing mirrors and filters in the path of a *parallel* beam minimizes image distortion.
[3] Emissivity is the ratio of thermal emission of an object to the emission of an ideal black body at the same temperature.

wavelength or temperature. In reality, the emissivity of many materials is not constant and incorrect temperature measurements result if a constant emissivity is assumed.[4] The emissivity of metals, for example, changes with wavelength, temperature, and the degree of oxidation. Glasses and plastics are transparent or translucent in some wavelength regions making measurements in those wavelength regions prone to large errors. Four spectrally-filtered images allow one to construct an algorithm that determines the emissivity and then, once emissivity is determined, temperature can be accurately calculated from the relative amplitudes of signals in each channel.

## Calibration

Pre and post-test calibrations were performed on both cameras. The calibrations included 1) image registration, i.e. the spatial relationship between the images on the CCD camera, 2) image magnification, and 3) background readings and their spatial variations. The end-to-end sensitivity with wavelength of each camera channel was determined prior to the campaigns by illuminating the front lens with a known amount of spectrally pure light (lamp light passed through a monochrometer) and recording it on the four frame camera's CCD. The channel sensitivities were then inserted into the data deconvolution software.

An additional calibration was performed to crosscheck the reduction algorithm. For this calibration a tungsten ribbon lamp was heated to a known temperature in the range of 2200 °K-2800 °K by passing through it a measured amount of current.[5,6] The hot ribbon

[4] E.D.Palik, *Handbook of Optical Constant of Solids*, Academic Press (1985); J.F.Chaney et al., *Thermophysical Properties Research Literature Retrieval Guide, 1900-1980*, vol.1-7, IFI/Plenum (1982).
[5] NRL Tungsten ribbon lamp #6858. The relationship between the ribbon's temperature and current was determined by the National Bureau of Standards (now NIST).

was then photographed by the four-frame camera and its temperature calculated using the four-frame camera's deconvolution algorithm with the channels sensitivities measured earlier. Then, the calculated temperature and the ribbon's actual temperature were compared for consistency. Results agreed to within 10%.

## *Spectrometer*

Emitted light from a 3-mm diameter spot on the front of the irradiated target was collected by a lens, imaged into a fused silica multi-mode fiber and delivered to a spectrometer and its detector. The detector was read out and recorded on the disk of a personal computer at a rate of 0.1 msec/spectrum. The spectrometer uses a 300 lines/mm grating and 50 micron slit, which provides spectral coverage from 500 nm to 1000 nm with 1-nm resolution. The spectrometer's data acquisition software was specially modified for this FEL experiment to allow rapid data acquisition. Special software was written, as well, to semi-automatically handle the large amount of data acquired, to convert the spectra to emission temperatures, and to produce a movie of the result.

The temperature of the imaged spot was calculated from the continuum part of the spectrum[7] by fitting its shape to the shape of a grey-body curve with temperature and the emissivity serving as free parameters. This technique was tested by NRL and was shown

---

[6] R. Stair, et. al., *Standard of Spectral Radiance for region of 0.25 to 2.6 um*, Journal of Research of the national Bureau of Standards - Physics and Chemistry Vol. 64A, No.4 July-August 1960; G.A.W. Rutgers et. al., *Relation Between Brightness Temperature, True Temperature, and Color Temperature of Tungsten*, Physica XX pg. 715-720.

[7] Any lines present in the spectrum are ignored. The lines, when present, correspond to the harmonics of the FEL laser beam.

to work well in the Defense Threat Reduction Agency's high explosive test Dipole Idle II, conducted at the White Sands Missile Range in 1995.[8]

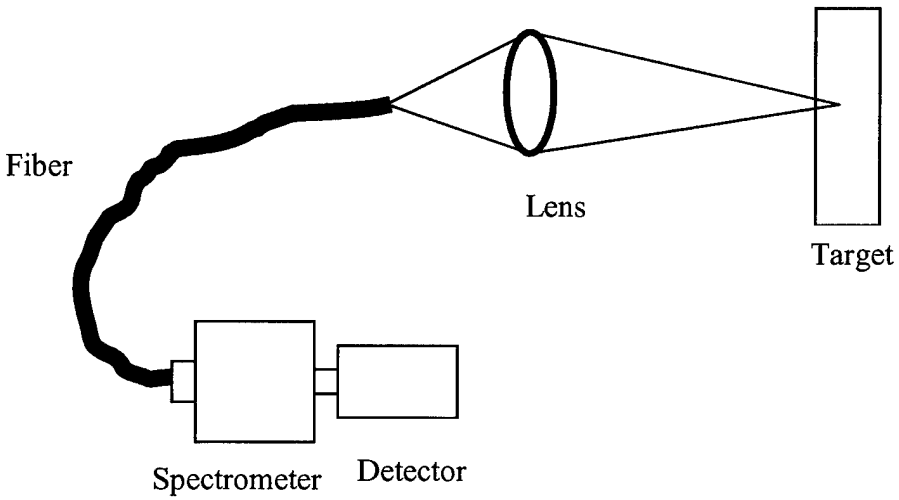


**Figure 2: Spectrometer setup. A lens images a 3-mm spot on the surface of an irradiated target onto the face of a spectrometer. The detector records the spectrum into a computer disk at a rate of 0.1msec/spectrum.**

## Calibration

The wavelength scale and wavelength sensitivity of the spectrometer was calibrated end-to-end, in-situ, at JLAB with a Pen-Ray Oriel spectral calibration lamp[9] and the tungsten ribbon lamp placed at the location of the sample. Wavelength calibration was obtained from the spectral-lamp lines and response as a function of wavelength from the known absolute emission of the tungsten lamp.

[8] C. Manka, *Light Intensity Data and Structure Interior in Dipole Idle-2,* Report to the L. Gilliam Division of Lockheed-Martin (1995).
[9] http://www.oriel.com/netcat/volumeiii/pdfs/v39pen.pdf

Figure 3 shows a typical result of the spectroscopy diagnostic. The data shown is from Suite 38-2, (target type 3)[10], illuminated with a 1000 Watt FEL beam operating at 37.4 MHz, and focused to produce 3 kW/cm$^2$ on the target surface. Shown are representative spectra, grey-body fits to the spectra, and the temperature history that was derived from the grey-body fits. The shot-to-shot reproducibility of the temperature is ± 10%, as shown in Figure 4.

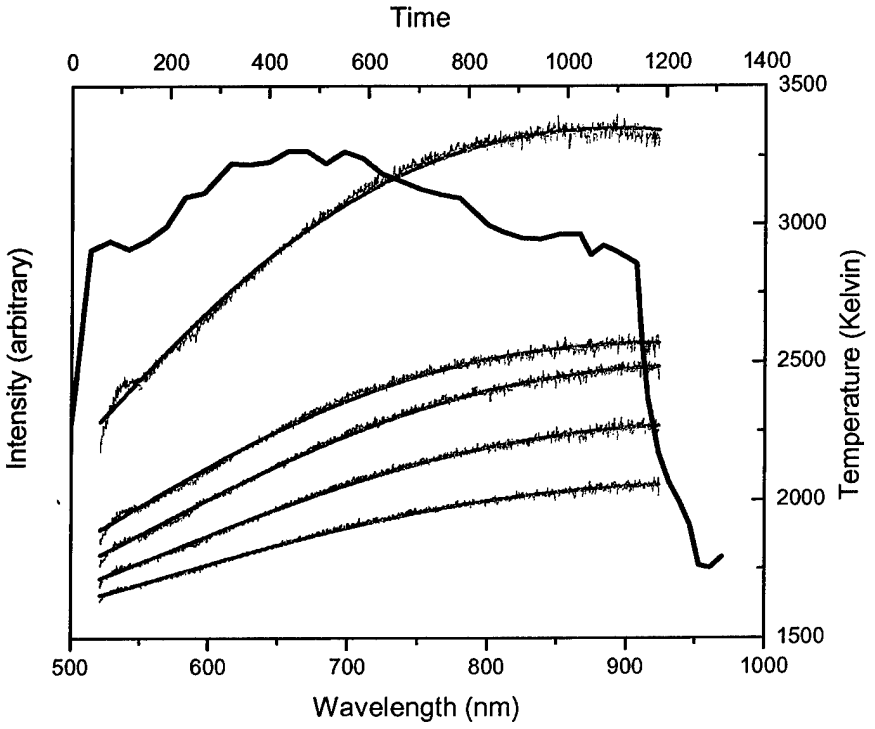


**Figure 3: How spectra are used to calculate temperature. Grey lines: Relative-time sequence of spectra and grey-body fits to the spectra from suite 38-2, target type 3, illuminated with a 1000 Watt FEL beam operating at 37.4 MHz, and focused to produce 3 kW/cm$^2$ on the target surface. The spectra shown are corrected for detector dark current and detector sensitivity. From bottom to top the times shown are 39 msec, 116 msec, 268 msec, 588 msec, and 869 msec. Heavy Black line: Temperatures as a function of time derived from the grey-body fits.**

[10] Proprietary samples in this report are designated as "target type #" in this report and are otherwise not precisely identified.

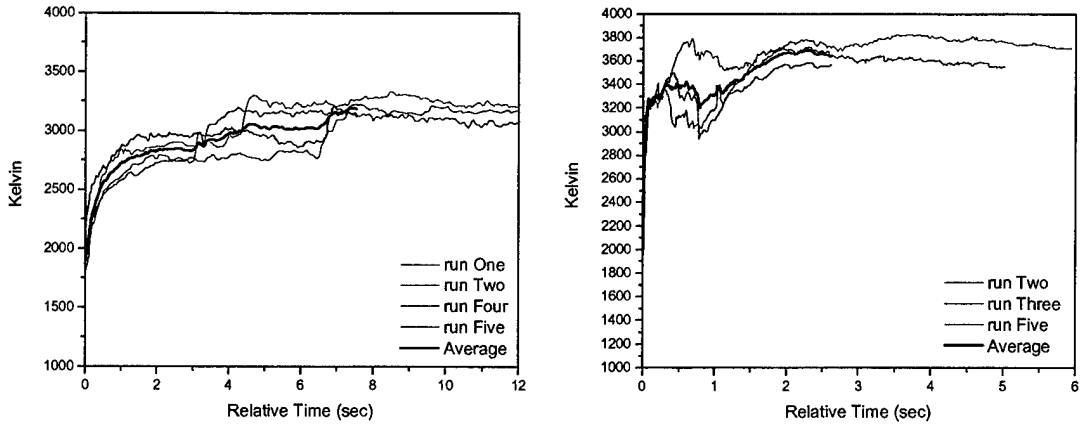


**Figure 4: Shot-to-shot temperature reproducibility: Left: Spectroscopically-determined time history of emission temperature of a 3 mm diameter spot on separate runs of suite 74, which consisted of a 1-inch diameter, 0.125-inch thick stainless steel sample illuminated by a 600 Watt FEL beam running at 74.85 MHz and focused to 3 kW/cm$^2$. Right: Spectroscopically-determined time history of emission temperature of a 3 mm diameter spot on separate runs of suite 67, which consisted of Target 2, a glass-cloth composite illuminated by a 600 Watt FEL beam running at 74.85 MHz and focused to 3 kW/cm$^2$. Individual temperature histories differ from their average by less then 10%.**

## *Interferometer*

To measure the density-above-ambient of material in front of the illuminated target we fielded a Mach-Zehnder[11] interferometer with a 30-mWatt, 0.532-micron wavelength laser to illuminate the target edge-on (Figure 1). A novel, state-of-the-art feature of the interferometer is the recording medium, an intensified, 18-mm diameter microchannel plate which can be gated to record a single frame with a minimum exposure time of 120-psec FWHM over the full cathode aperture. The microchannel plate uses an entirely solid-state electronic pulser to give ultra-fast gating speeds with a jitter of less than 20-psec RMS, combined with a small trigger delay, typically 18 ns plus cables. The gate can be triggered externally and thus synchronized with a particular pulse of the FEL, thereby

[11] M. Born and E. Wolf, *Principles of Optics*, (Pergamon Press, New York, 1975).

allowing determination of the density of material in front of the target at a given time after a particular FEL pulse. Thus, the diagnostic can measure the formation, persistence, and dissipation of plumes in front of the target. Typical spatial resolution at the intensifier is 10 lp/mm. The intensified image is read out with a CCD camera and recorded.[12]

## Interpretation

Determining density with an interferometer requires paying attention to the following set of equations and considerations.

Upon passage through a gas the diagnostic laser undergoes a shift of phase $\Delta\varphi$ radians, given by

$$\Delta\varphi = \frac{2\pi(\nu-1)}{n_0\lambda}\int_0^L n_{neutral}dx - \frac{e^2}{mc^2}\lambda\int_0^L n_{electron}dx$$

where $\nu$ = index of refraction of the neutral gas at density $n_0$, $\lambda$ is the wavelength of the probing laser, L is the distance through which the probe propagates, e is the electron charge, m is the electron mass, and c is the speed of light in vacuum. The quantities $n_{neutral}$ and $n_{electron}$ are the densities of the neutral atoms and $n_{electron}$ is the density of free electrons. The free electrons exist if the temperature is high enough to ionize the gas.

[12] One frame is acquired on each test. We have the capability to set up a version of this diagnostic that acquires eight frames on each test.

For our experiment, which is performed in air at 1 atmosphere pressure and room temperature, $\nu$-1 = 2775E-7, $n_0$ = 2.7E19 $cm^{-3}$, $\lambda$= 0.53μm, and $e^2/mc^2$ = 2.82E-13 cm.[13] L is of order of the FEL focal spot diameter, generally a few millimeters.

In what follows below we will write $n_{electron} = I\ n_{neutral}$, where I is the number of free electrons for each initially neutral atom, and rewrite two components of the equation above as

$$\Delta\varphi_{neutral} = \frac{2\pi(\nu-1)}{n_0\lambda} n_{neutral} L$$

$$\Delta\varphi_{electron}(I) = \frac{e^2 I}{mc^2} \lambda n_{neutral} L$$

$$\Delta\varphi = \Delta\varphi_{neutral} - \Delta\varphi_{electron}(I)$$

Assuming L is known, then in neutral gas, where I = 0, the phase change is a direct measure of neutral density, otherwise the phase change is a mixture of the contributions of phase changes from neutral species and free electrons. (A possible contribution to the phase change by resonant interaction with bound excited electrons is neglected in this analysis.)

To estimate the sensitivity of phase change to free electron contributions we evaluate the ratio $\frac{\Delta\varphi_{electron}(I)}{\Delta\varphi_{neutral}}$ for different values of I, and determine that

$$\frac{\Delta\varphi_{electron}(0.01)}{\Delta\varphi_{neutral}} = 0.12$$

[13] *CRC handbook of Physics and Chemistry*, 2001 edition, page 10-220

$$\frac{\Delta\varphi_{electron}(0.09)}{\Delta\varphi_{neutral}} = 1.1$$

$$\frac{\Delta\varphi_{electron}(1)}{\Delta\varphi_{neutral}} = 12$$

That is, for ionization I less than 1% the measured phase is due primarily to neutral atoms. For I greater then 100% the measured phase is due primarily to electrons. Otherwise both terms must be taken into account and the neutral density calculated from relationships between level of ionization and gas conditions.

To see whether electrons must be taken into account in this experiment we will estimate the degree of ionization from the temperature of the gas, which we will take to be the same as the temperature of the heated target.

The relationship between temperature T and the degree of ionization I is estimated from the following table[14] valid for air at standard density, assumed to be composed of nitrogen and oxygen only.

| Temperature in Kelvin | Degree of ionization I |
|---|---|
| 293 | 0 |
| 20,000 | 0.24 |
| 50,000 | 1.5 |
| 100,000 | 2.65 |
| 250,000 | 5 |
| 500,000 | 5.2 |

**Table 1: Calculated relationship between a nitrogen-oxygen atmosphere and degree of ionization.**

A linear interpolation between 293 °K (room temperature) and 20,000 °K, I = 1.22E-5 T (Kelvin) – 3.57E-3, gives

[14] Table 3.3 in Ya. B. Zel'dovich and Yu. P. Raizer, *Physics of Shock Waves and High-Temperature Hydrodynamic Phenomena*, (Academic Press, New York, 1967).

I = 0.01 at ~ 1,000 °K
I = 0.02 at ~ 2,000 °K
I = 0.03 at ~ 3,000 °K
I = 0.09 at ~ 7,700 °K
I = 1 at ~83,000 °K

Thus, at 1000K electrons contribute 10% to the measured phase and hence 10% to the error in determining density of neutrals. At 2000K, the error is about 25%, and at 3000K 37%. (If better accuracy is required a "two color" version of the Mach-Zehnder interferometer, which distinguishes neutrals from electrons, can be used.)

# Results

## *Stainless Steel*

A typical sequence of spatial temperature profiles on the front surface of a 304 alloy stainless steel alloy is shown in Figure 6. Here, the sample (suite 48-2) was a 1-inch diameter, 0.0625-inches thick steel disk illuminated by a 300 Watt, 18.7 MHz FEL beam focused to 3 kW/cm$^2$ for 15 seconds. The first few frames do not show any image since the temperature of the sample is below the threshold of 800 °K that can be measured by the camera in its current configuration.[15] By frame 5, arbitrarily designated to be 0 sec, a small, 3-mm diameter spot with a nearly uniform flat-top temperature profile of about 1500 °K appears. The heated spot grows in diameter until, at 10 seconds, it reaches a diameter of 6mm, still exhibiting a horizontally flat temperature profile of about 1500 °K. Afterwards the spot begins to shrink as the laser is turned off, until it reaches 2.4-mm diameter at 13 sec. Then, the temperature again falls below the measurement threshold of the camera.

[15] The temperature threshold can be lowered by appropriate choice of narrow band filters and recording medium.

It is interesting to note that although the incident laser beam has an approximately Gaussian shape (Figure 5), as measured by a time-integrating CCD camera, the resulting temperature profiles are mostly flat and show that a uniform heat load on the sample can be obtained even with a non-uniform laser beam. This phenomenon is probably due to the temperature becoming clamped in the melting temperature range of 304 alloy stainless steel, which is (*solidus* to *liquidus*) 1672 °K to 1727 °K.[16,17]

**Figure 5 Focal spots on 6 successive exposures of Suite 48. Nominal focal spot diameter is 3.5 mm.**

[16] *Aerospace Structural Metals Handbook*, AFML-TR-68-115, Code 1303, page 1, (1972).

[17] Alloys, being a mixture of elements, melt over a temperature range rather than at a single temperature. The heat of fusion is absorbed incrementally with temperature in a not well known manner. The *solidus* temperature is where the alloy first starts to melt (usually at grain boundaries where the minor constituents are concentrated). The *liquidus* temperature is where the all the constituents of the metal are in a liquid mélange.

Also visible in these pictures at times of 3.6 seconds to 6.4 seconds is an asymmetry in the heated spot, a protrusion of mostly 1500 °K material at about 11 O'clock, which we believe represents material flowing out of the heated spot under the influence of the Mach 0.1 airflow.

Although the temperature profile is mostly flat, a thin region near upper edge of the image tends to be much hotter, reaching temperatures of up to 3000 °K, as shown in the graph on Figure 6. This temperature corresponds closely to 3020 °K, the textbook value for the boiling temperature of iron[18] – the major constituent of steel. Through most of the exposure, including the beginning, the hot region is just a sliver at the edge of the hot spot. Towards the end of the exposure, however, the hotter region occupies a more significant portion of the spot. At 13 seconds, as the spot is getting smaller due to the laser being shut off, roughly its upper one-half is hotter than 1500 °K.

It is quite possible that the presence of a hot upper lip and the presence of material flow in roughly the same direction are related. Suppose, for instance, that the molten material being pushed out of the heated spot by the airflow does not maintain good thermal contact with the cooler and now shadowed surface of the sample, but that it is still being irradiated by the outer edges of the approximately Gaussian laser beam. Then, the molten material would continue to absorb laser energy without being able to shed thermal energy via conduction into cooler parts of the metal. Enough energy could be trapped in this manner to raise the molten metal to liquid and then vaporization temperatures.

[18] *CRC Handbook of Materials Science*, Vol. I: General Properties, CRC Press Inc., Boca Raton, Florida, pp 24, (1974).

It is also possible to raise the sample temperature above its melting region by restricting heat flow from the entire sample or by heating it with more power than can be dissipated. For example, spatially-averaged heated spot temperatures calculated from emission spectra show that 1-inch diameter samples irradiated with 300 Watts reached the melting temperature of steel. But, smaller-diameter samples thermally isolated from their surroundings reached higher spatially-averaged temperatures under similar irradiation conditions. One example of this is shown in Figure 8, where we compare temperatures reached by a standard 1-inch diameter steel sample to a special case of a 0.25 inch (0.125 inches thick) diameter sample. Both samples were irradiated at 300Watts, with a 74.85 MHz repetition rate and a focal spot designed to give 3 $kW/cm^2$. Even though the smaller-diameter sample was irradiated for only $1/5^{th}$ the time of the larger-diameter sample, it reached an average temperature of at least 2200 °K, 30% higher than temperature of the 1-inch diameter sample. The 30% or greater temperature difference is a measure of the effect that thermal conduction has on the irradiation of large diameter samples.

Another example, also in Figure 8, compares the spatially-averaged temperature of standard 1-inch diameter (0.125" thick) stainless steel sample, suite 74-1, irradiated with 600 Watts instead of 300 Watts. Its average temperature rose to the boiling temperature of iron, ~3000 °K. It was not obvious from a visual inspection of the samples which was heated to a melting and which to a boiling temperature. (Parenthetically, it seems the energy used to boil the steel is wasted since melting the steel would be good enough to damage the sample.)

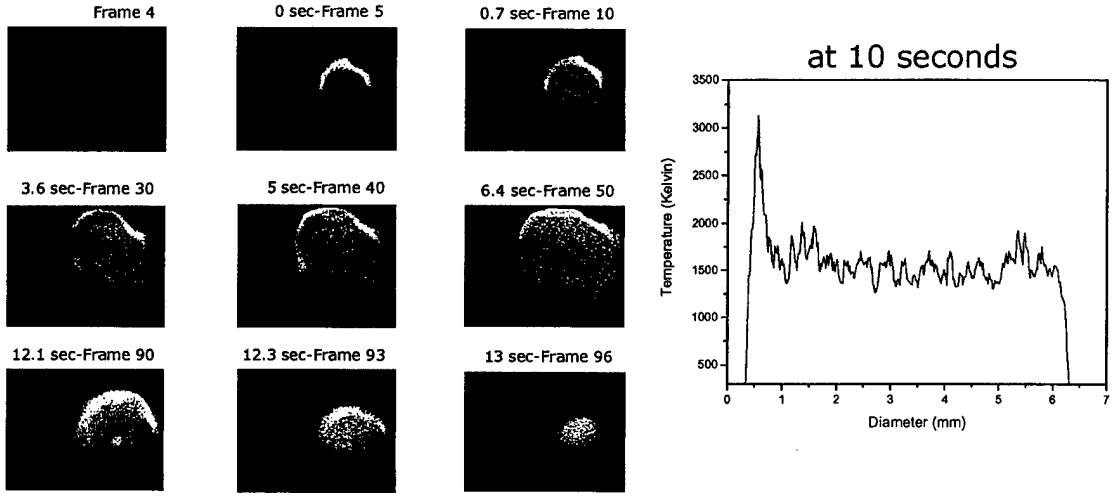


**Figure 6 Temperature profiles on the front surface of a 1-inch diameter, 0.0625-inches thick stainless steel disk illuminated by a 300 Watt, 18.7 MHz FEL beam focused to 3kW/cm$^2$ for 15 seconds (suite 48-2).**

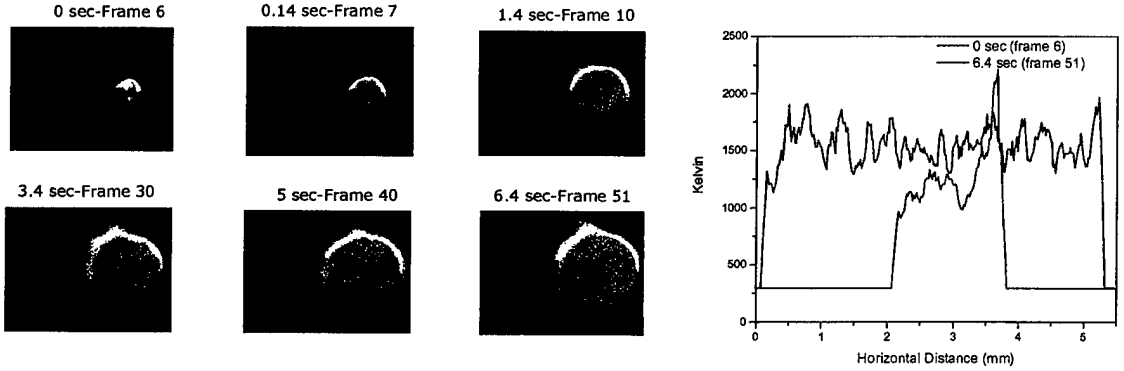


**Figure 7: Temperature profiles on the front surface of a 1-inch diameter, 0.0625-inches thick stainless steel disk illuminated by a 300 Watt, 18.7 MHz FEL beam (suite 49-1).**

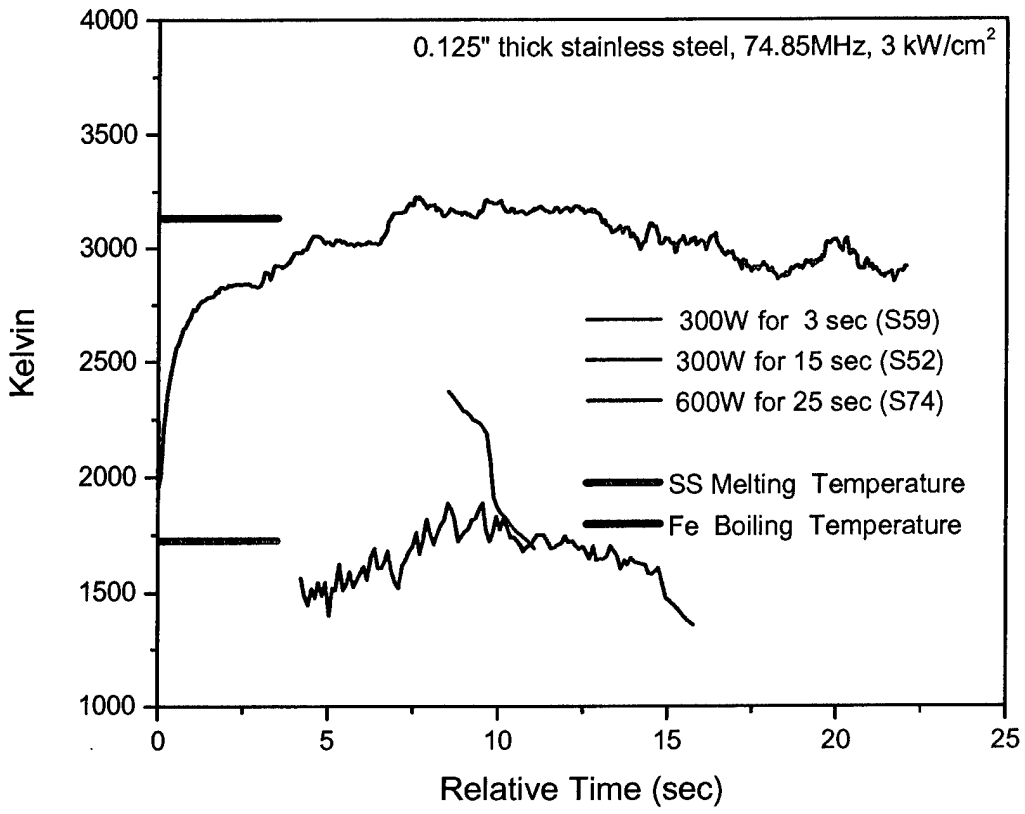


**Figure 8: Spatially-averaged front surface emission temperatures of three 0.125" thick stainless steel samples exposed to a 74.85 MHz FEL pulse train focused to produce 3 kW/cm$^2$ on the sample surface. The sample labeled S52 (i.e. suite 52) had a 1-inch diameter and was exposed with an FEL power of 300 Watts. Sample S59 was exposed at the same power for 1/5$^{th}$ the time yet it reached a temperature approximately 30% higher then the melting temperature of steel. The diameter of this sample was 0.25 inches. Sample S74 had a diameter of 1 inch but was irradiated at 600 Watts. It reached a temperature equivalent to the boiling temperature of iron, the main constituent of stainless steel.**

Besides measuring the emission temperature profiles on the front, laser illuminated, side of the target it is also possible to measure temperature profiles on the back of the target and to watch the target melt and burn through. This type of measurement, when temporally synchronized to the same diagnostic on the front of the target, can be used to measure burnthrough times and heat conduction. Without synchronization, the dimension of the heated spot as a function of target thickness, and a measurement of what happens to the melted material at the target back (ex. resolidification causing hole

closing) is possible. Camera synchronization necessary to perform burnthrough measurements has not been done in this experiment, but data at the target rear independent of data at the target front have been taken. Figure 9 shows such data, here suite 90-2, stainless steel irradiated with a 650 Watts, 74.85 MHz FEL focused to produce 0.5 kW/cm$^2$. The data shows a flat temperature profile at the rear of the target - initially in a small spot, the spot growing in size, until eventually, at 5.7 seconds, a hole is burned through the steel. The melted material from within the hole drips down the rear side of the target eventually forming two hot nodules that resolidify in place and disappear from the image. The shapes of the hole as well as the resolidified nodules are comparable to what is observed on the exposed samples after the experiment.

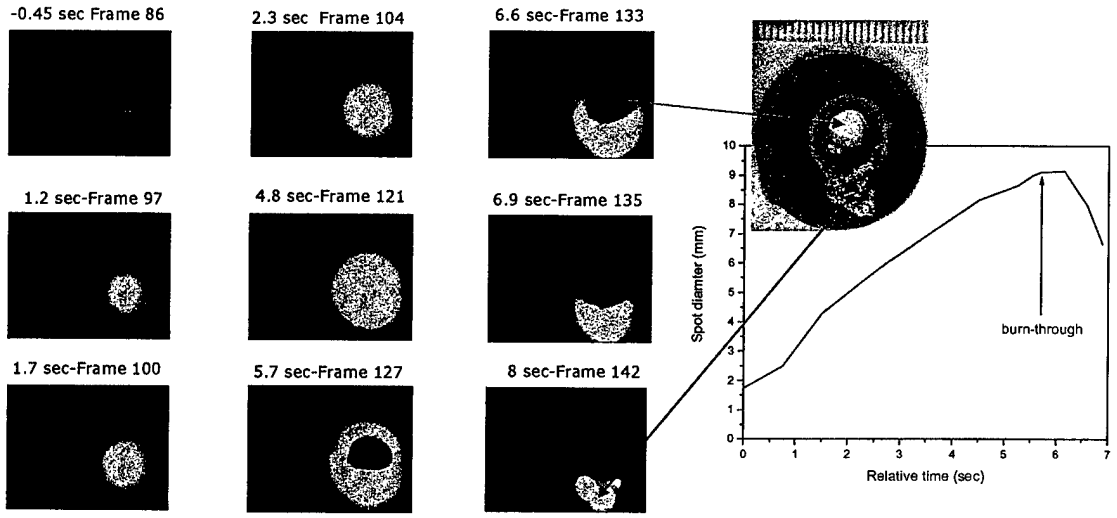


**Figure 9: Emission temperature at the rear surface of a stainless steel target, suite 90-2, exposed by a 74.85 MHz, 650 Watt FEL pulse train focused to produce 0.5kW/cm$^2$ on the target surface. The hot spot diameter at the rear grows from an initial 1.7mm to 8mm at the moment of burnthrough. The asymmetry in the hot spot after burnthrough is caused by molten material dripping down the target rear.**

Stainless steel Q*s for samples exposed at 1 kWatt/cm$^2$ were 12 kJoule/gm, much higher than the 4.4 kJoule/gm typically measured at similar irradiances and wavelengths on lasers other than the FEL.[19] The most likely explanation for this is that the FEL, having an output of ~ 1 kWatt, had to be focused to small spot sizes to produce the stated irradiance, and lateral thermal conduction played a significant role. Q* of 4.4 kJoule/gm were measured with 10-100 kWatt lasers focused to larger spots so that thermal conduction played a smaller role.

Everything presented thus far quantifies and is in accord with intuitive expectations. But, this it not true for all the cases examined. In fact, many of the exposures of stainless steel exhibited not the uniform emission temperatures profiles of Figure 6, but highly nonuniform bagel-shaped profiles, such as those shown in Figure 10. At times, a uniform temperature profile acquired during the exposure of a target within a particular suite was immediately followed by a bagel shaped profile on the very next target exposed. One would to ascribe the bagel-shaped nonuniformities on illumination by a similarly shaped laser beam profile. In fact, the bagel shape is highly reminiscent of the first peak in a diffraction pattern caused by a circular aperture somewhere in the laser beam path. A beam which wanders into such an aperture either because it or the aperture is misaligned will cause such shapes. This is often observed, for example, in glass lasers. But, in these experiments, the laser spot was monitored on each shot by splitting-off a piece of the beam with a partially reflective window and recording the split-off part on a time integrated camera. On these time integrated pictures a hollow beam profile needed to

[19] Private communications from multiple sources to R. Wenzel.

produced the observed temperature results was not seen. Thus, while it is possible that time-resolved measurements would reveal a hollow profile during some portion within the laser pulse train, the reason for the observed hollow temperature profiles remains a puzzle.

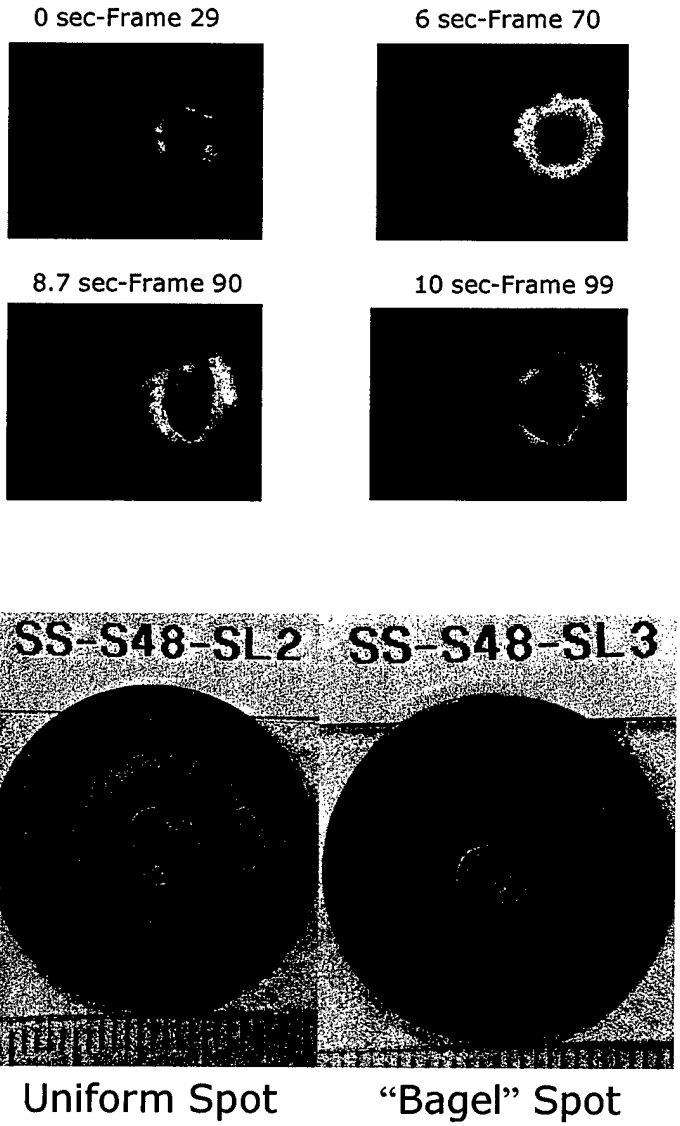


**Figure 10: Top: Bagel-shaped emission temperature profile measured on suite 48-3. The illumination conditions on this target were 300W, 18.7MHz repetition rate, and an irradiance of 3kW/cm$^2$. Bottom: Melt pattern exhibited on target 3 of suite 48 looks different than the melt pattern of target 2 of the same suite. Target 2 temperatures were spatially uniform and target 3 temperatures were bagel-shaped.**

## *Aluminum*

Experience with infrared CW lasers at less than 50 kW/cm$^2$ indicates that painted samples damage more severely that unpainted ones.[20] This is because unpainted samples reflect much of the incident laser energy, having only 3-7% absorption at 3 microns, thereby experiencing a lower thermal load than they would experience if most of the laser energy was absorbed. A less than 50 kW/cm$^2$ infrared CW laser, when irradiating a painted metal surface, first cooks the volatile gases out of the paint, leaving a paint residue, which is highly absorbing (50% to 80%). Carbon char and pigment in the paint absorb the laser energy which is then conducted to the underlying aluminum, causing the aluminum to melt. The paint residue adheres tenaciously to the metal, and is not removed by high-velocity airflow. The paint residue in aluminum even affects molten metal in the absence of strong airflow; it seems to be incorporated in the molten layer providing the surface tension, which prevents the metal from flowing out of the target. At more than 50 kW/cm$^2$ the paint is more cleanly removed and painted and unpainted aluminum have similar penetration times.

A conventional, pulsed, non-FEL laser meant for directed energy lethality typically has pulse durations of hundreds of nanoseconds to many of microseconds, a 100-1000 Hz repetition rate, and delivers on the order of joules per pulse. Because of the low repetition rate each pulse must itself cause significant damage and thus is focused to joules/cm$^2$ per pulse – and peak irradiances of order $10^2$-$10^5$ kW/cm$^2$. At such irradiance levels, a single laser pulse, or a few pulses cleanly remove all the paint from a sample

[20] R. F. Wenzel, *Pulsed Laser Lethality Assessment*, Naval Research Laboratory Memorandum NRL/MR/6330—02-8619 (2002).

surface, leaving bare metal behind. Thus, subsequent pulses suffer from the high reflectivity the first few pulses created. What happens when painted aluminum is exposed to an FEL laser is not *a priory* clear. An FEL's pulse duration is of order of a picosecond, its repetition rate is tens of MHz, it delivers fractions of a millijoule per pulse, and it is focused on the sample surface to $mJ/cm^2$ per pulse. At less than 50 $kW/cm^2$ average irradiance, the FEL's peak irradiance can be hundreds of $kW/cm^2$. An FEL pulse used in a directed energy weapon configuration, therefore, can have average power characteristics of a low power CW laser – and not remove paint efficiently - and peak power characteristics of a conventional pulsed laser – which cleans paint effectively. Which is it?

To answer this question, experiments using 10 $kW/cm^2$ average irradiance and $10^5$ $kW/cm^2$ peak irradiance were performed on unpainted Aluminum (6061 alloy) samples and on Aluminum samples painted with the current Navy aircraft paint process of a chromate conversion coating, primer and gray topcoat.[21] Post-shot examination of the samples indicates that the paint char remains on the aluminum causing enhanced absorption and more serious damage. This can be seen in a post-irradiation examination of painted and unpainted Aluminum samples such as the ones shown in Figure 11. Time-resolved temperature profile measurements likewise show that the painted target reached a temperature of ~1800 °K while the unpainted target reached a 20% lower temperature of ~ 1500 °K. Both temperatures are higher than the melting temperature of aluminum

[21] The samples were cleaned, degreased, deoxidized and chromate (Alodine 1200S) pretreated, primed with MIL-PRF-85582C, Type II Class C2, and topcoated with MIL-PRF-85285C, Type I, Gray color 36375. The total dry film thickness is on the order of 0.002".

which is about 1000 °K, but lower than the boiling temperature of about 2800 °K (Figure 12).

The painted aluminum sample was irradiated into oblivion, by a large overestimation of the time required to damage. The remaining molten aluminum coalesced under surface tension in the rearward region where there was little or no airflow. In the case of the bare aluminum the heating was slower. A hole probably formed in the sample, but then filled as the melt slumped on the back under gravity. About one half of the sample was in the flowing melt stage. The surface was heavily oxidized, as shown by the shiny unoxidized aluminum revealed in the cooling cracks. The rear shows an area seemingly spray-painted white. This is probably vaporized and re-deposited, MgO, as magnesium is present in the alloy at the 1 percent level, and readily oxidizes. Later experiments, when the irradiation time was considerably reduced, the bare aluminum appeared to be untouched, while the painted sample showed considerable melting damage. Thus, at the 10 kW/cm$^2$ and lower level, the FEL laser behaves as a CW device.

Q*s on bare Aluminum samples for samples exposed at 1 kWatt/cm$^2$ were 27 kJoule/gm, compared to 11.5 kJoule/gm typically measured at similar irradiances and wavelengths on lasers other than the FEL.[19] The explanation for the discrepancy is the same as the one given earlier for the steel samples.

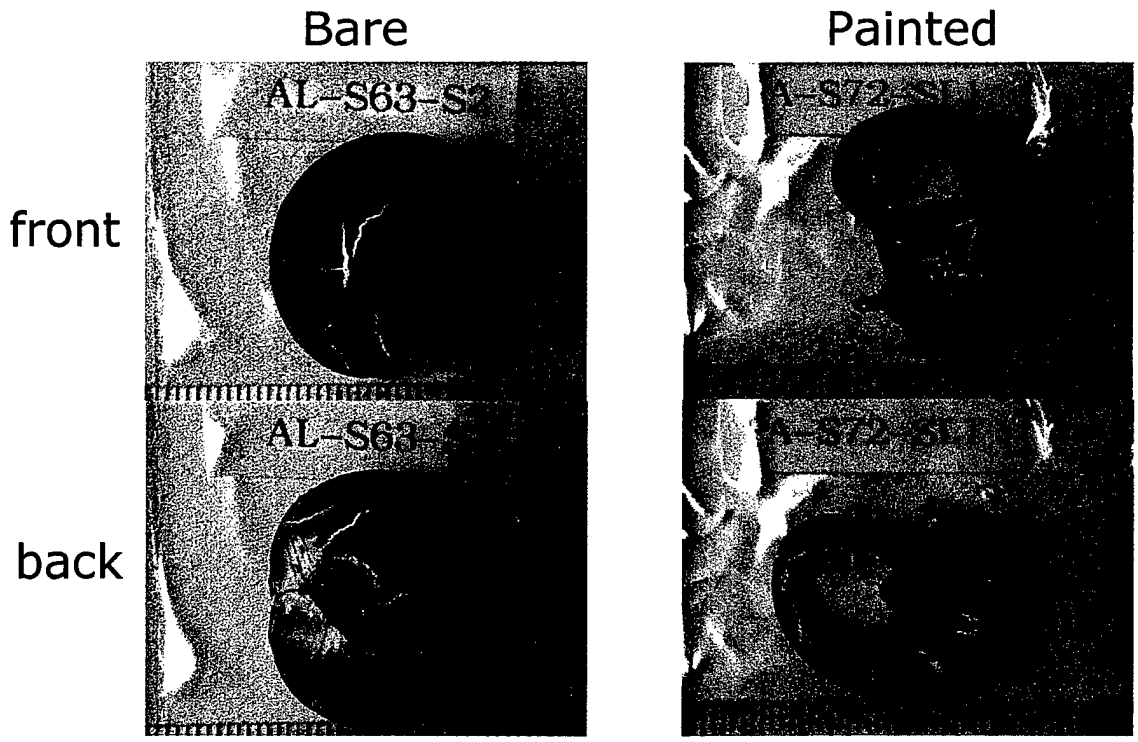


**Figure 11: Damage to unpainted and painted aluminum samples suite 63-2 (unpainted) and suite 72-1 (painted with Al 2024-73). Both samples were illuminated with a 600 Watts, 74.85 MHz laser beam focused to 10kW/cm$^2$. The samples were irradiated for 20 and 15 seconds for the bare and painted, respectively.**

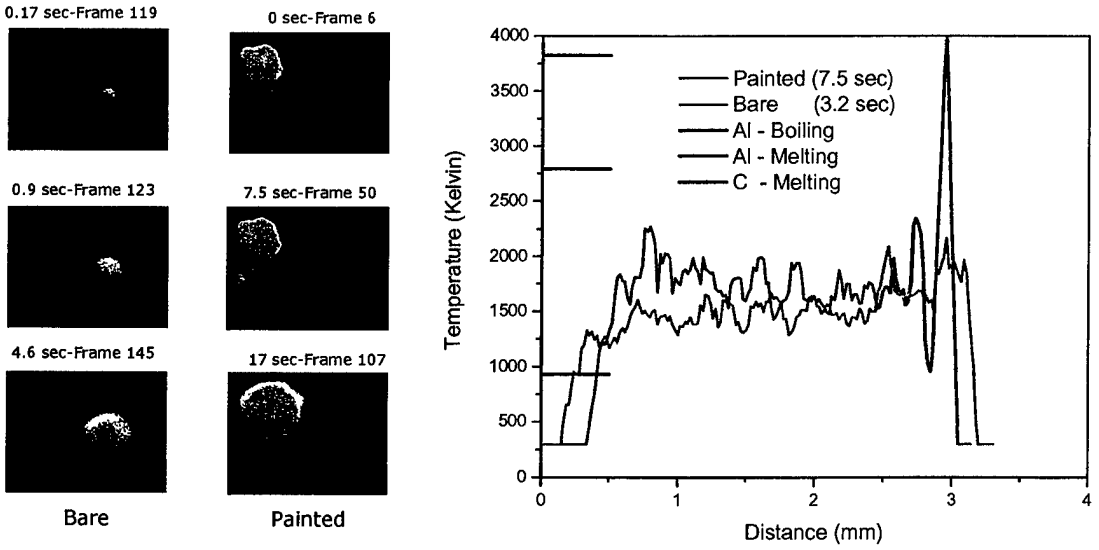


**Figure 12: Temperatures of painted and unpainted aluminum samples in Figure 11.**

## *Organic Glass Composite*

A radome material composed of a glass cloth held together by an organic resin, labeled "Target type 2" in these experiments was tested. The probable damage sequence for this material, at least when irradiated with a CW laser, is as follows:[22] First, energy is absorbed by the organic resin within target. The resin vaporizes, producing carbonized char which further absorbs and heats. At temperatures of 573 °K to 750 °K the resin cooks-out from between the fibers of the glass-cloth weave. Forty percent of the mass in the target is lost between the temperatures of 573 °K and 673 °K, and another fifteen percent between 673 °K and 750 °K (Figure 13). The carbon char itself sublimes at 3640 °K.[23] The carbon is hotter than the supporting glass fiber can tolerate, so the fiber melts as the carbon on its surface sublimes.

Figure 14-Left shows a frame from a time sequence of measured emission temperatures on "Target type 2" (suite 29-2) when irradiated by a 1000 Watt, 74.85 MHz FEL pulse train focused to 10 kW/cm$^2$. The 1-mm-weave of the glass cloth of the target and the organic resin in between the glass fibers are clearly visible in the photograph and from the temperatures of each one can infer the process occurring at the time the image was taken. For example, the black region on the image designate temperatures lower than about 700 °K, indicating the locations of resin cook off. Dark grey region are ~950 °K and light grey about ~2500 °K. White regions, which register at ~4000 °K, are region

[22] R. Cozzens, R. Wenzel, J. Cook, C. Lloyd, S. Jensen, and T. Schriempf, *Laser Induced Char Effects on Missile Radomes,* 5th National Meeting, Directed Energy Professional Society, Monterey, CA, Nov 2002; The degradation sequence was measured using relatively slow heating. Rapid heating with a pulsed laser may, possibly, give somewhat different results.

[23] The char (carbon) sublimes before it melts; the melting temperature of carbon is about 3820 K.

where the carbonized char is sublimating. The spatially-averaged temperature of the target, measured with our spectrometer is 2900 °K. For comparison, photographed images of the damaged target are shown in Figure 14-Right.

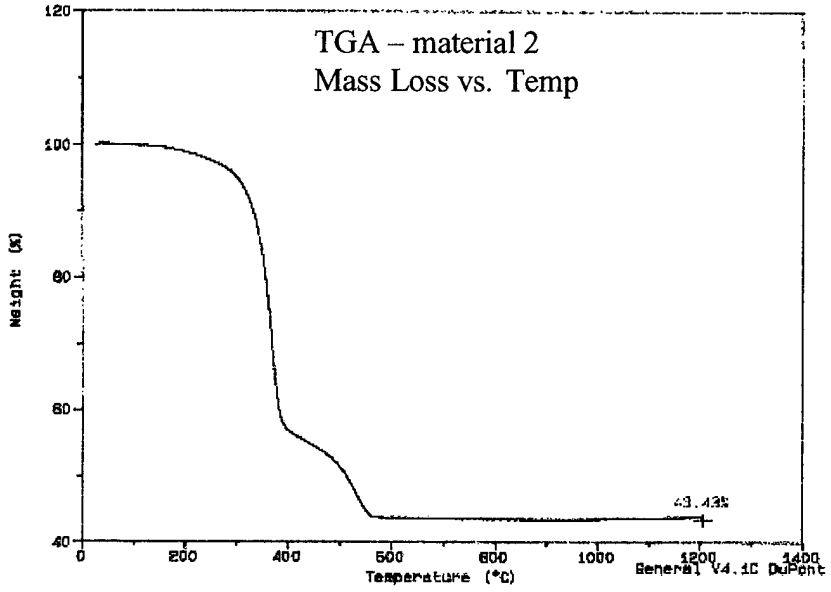


**Figure 13: Mass loss versus temperature in target 2 heated in an oven.**

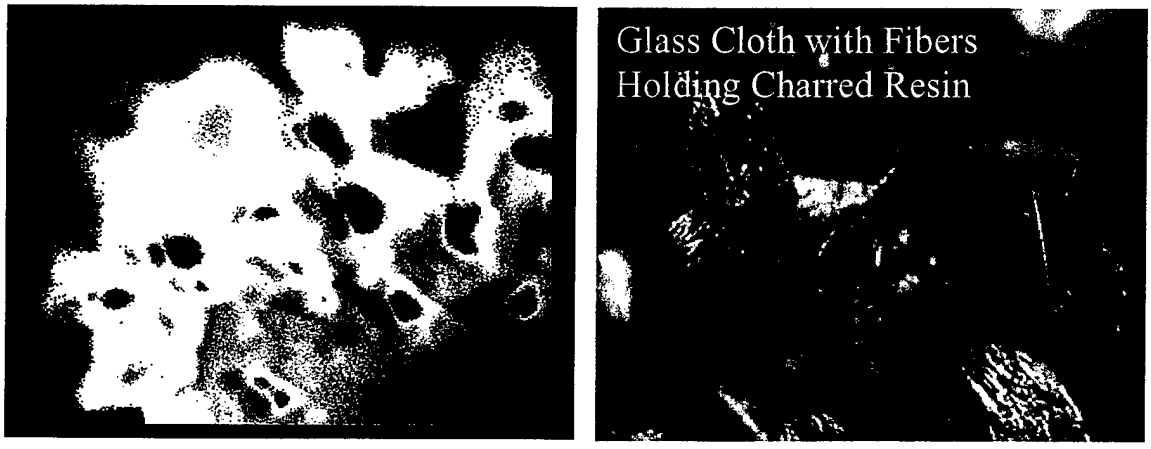


**Figure 14: Left: Temperature profile of "Target type 2" when irradiated by a 1000 attW, 74.85 MHz FEL pulse train focused to 10 kW/cm$^2$ (suite 29-2). Black regions on the image indicated temperatures lower than about 700 °K, indicating the locations of resin cook off. Dark grey regions are ~950 °K and light grey about ~2500 °K. White regions, which register at ~4000 °K, are region where the carbonized resin (char) is subliming. Right: An optical image of same target after the shot showing remnants of the glass cloth held together by carbonized char. Glass fibers in both images are 1 mm apart, giving the approximate scale in both images.**

A time sequence of the emission temperatures of "Target type 2" exposed at a lower irradiance of 0.5 kW/cm$^2$ is shown in Figure 15. The target in this case, suite 89-6, was exposed by an FEL run at 650 Watts and 74.85 MHz. The time sequence shows the evolution of temperature through to hole-burning and the separation of individual strands of glass from the bulk of the target. At about 10.4 seconds after the appearance of the first image the average temperature on the target surface is ~1750 °K.

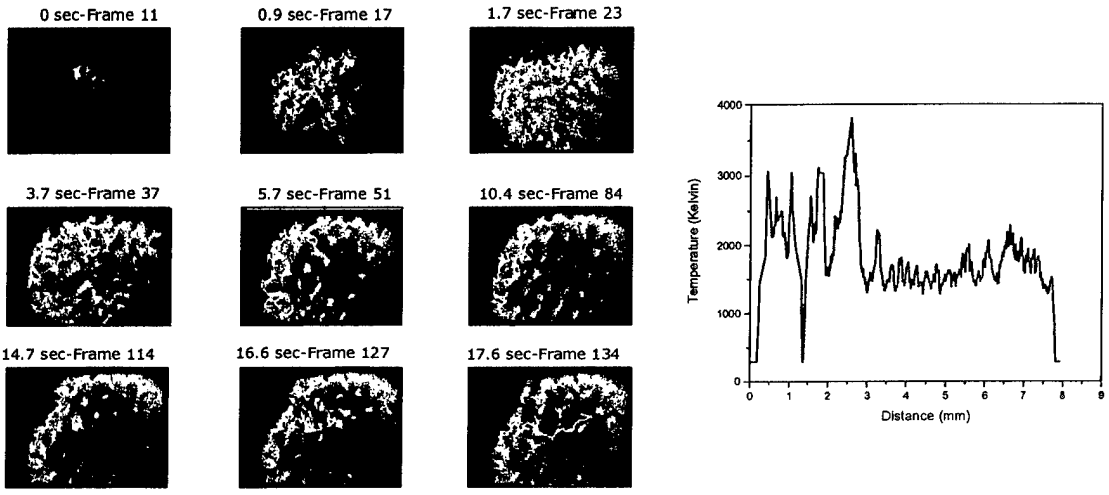


**Figure 15: Left: Time sequence of the emission temperatures of "Target type 2", suite 89-6, exposed by an FEL run at 650 Watt and 74.85 MHz and focused to 0.5 kW/cm$^2$. Right: Temperature scan across the horizontal center of frame 84.**

## *Pyroceram & SCFS*

A Pyroceram radome-like material was tested under illumination conditions identical to certain illuminations of the organic glass composite. The sample showed melting occurring in the illuminated region and, interestingly, cracks propagating in opposite direction from within the melted region. Spatially-averaged but time-resolved temperature measurements indicated that the front surface was about 2800 °K,

significantly higher than the Pyroceram melting temperature of 1620 °K or even the Pyroceram vaporization temperature of 2200 °K. This temperature was also similar to the front-surface temperature measured on the glass composite under the same conditions (Figure 16). The temperature, however, was lower than that of identically illuminated slip-cast fused silica (SCFS) $SiO_2$ radome-like material on which we measured spatially-averaged temperatures of 4100 °K ± 5%. As is the case with Pyroceram, these temperatures are much higher than either the melting, (1980 °K) or vaporization (2300 °K) temperatures of SCFS. Unlike Pyroceram, SCFS showed no signs of cracking or damage far outside the focal region. Within the focal region solidified liquid $SiO_2$ droplets arranged in a pentagonal structure (Figure 17) were observed. A time sequence taken by the 4-frame camera captured these droplets in the process of formation, while they are still in a liquid state. The behavior of the liquid droplets seen on the 4-frame camera is reminiscent of Benard convection cells observed, for example, in cooking liquid.

Q* measured on SCFS at 1 kWatt/cm$^2$ were unusually high, at 550 kJoules/gm, compared to 12 kJoules/gm measured on other non-FEL lasers.[19] Thermal diffusion from small spot sizes is an unlikely explanation for this large discrepancy since thermal conductivity for non-metallic samples is much smaller than for metallic samples such as aluminum and steel. (Furthermore, on other types of non-metallic samples irradiated at 1kJoule/cm$^2$, such as Plexiglass, Q*s of 3 kJoule/gm were the same for this FEL and non-FEL lasers.) Rather, the explanation here is that in the absence of strong airflow molten SCFS resolidifies on the sample surface causing erroneous inferences of Q* from measurements of removed mass.

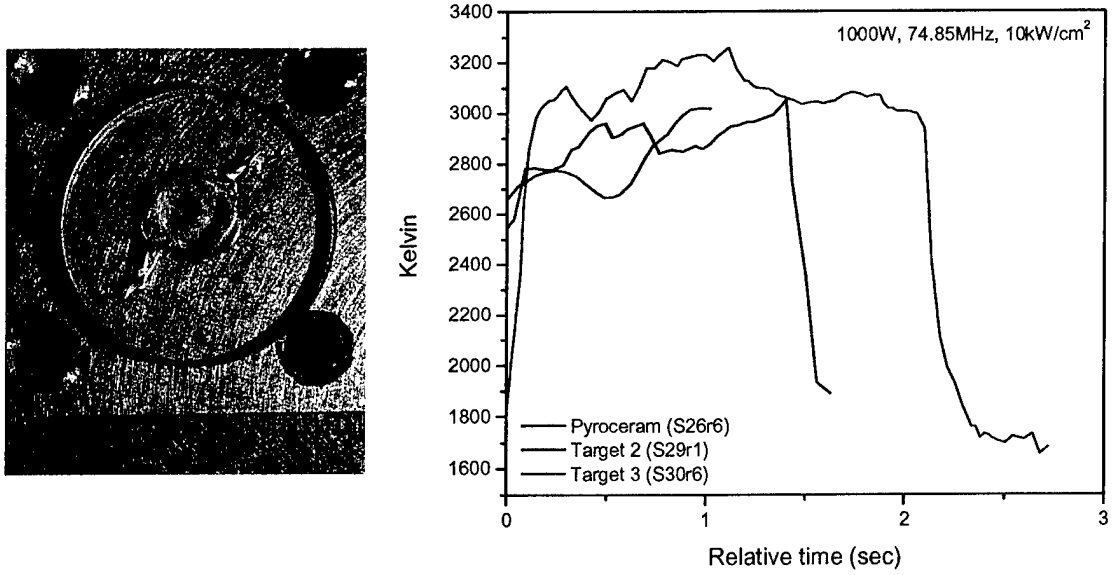


**Figure 16: Left: Pyroceram target (Suite 26-6) after irradiation at 1000 Watt, 74.85 MHz, and 10 kW/cm$^2$. Damage in the form of cracks propagating in opposite directions extends beyond the irradiated spot. The scale divisions in the photograph are millimeters. Right: Time-resolved temperatures of the Pyroceram target on left compared to those from Target type 2 irradiated under the same conditions (Suite 30-6 and Suite 29-21).**

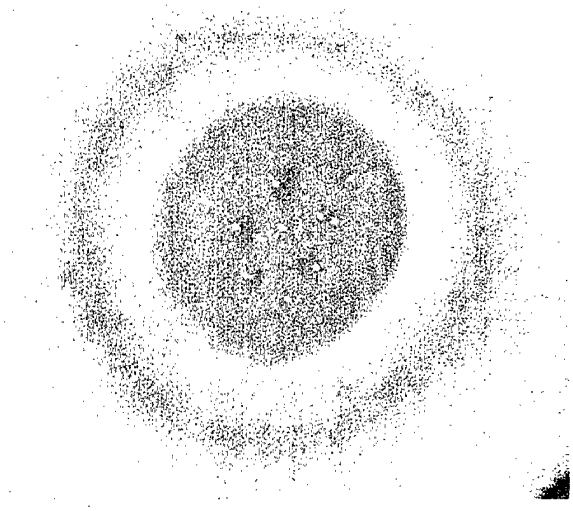



**Figure 17: Bubbles of liquid $SiO_2$ frozen solid after irradiation with a 1000 Watt, 74.8 MHz, 10 kW/cm$^2$ FEL pulse train. The formation of these bubbles while they are still in the liquid state was measured with the 4-frame imager.**

## Plumes

The utility of the plume interferometry diagnostic in this experiment depends on its ability to be synchronized with a particular pulse of the FEL. If this were done, then it would be possible to map the evolution of a plume after the target is irradiated by a particular FEL pulse. The lack of an appropriate trigger from the FEL made this experiment impossible to do, so the interferometry data we acquired are taken at an unknown time during the exposure of the target. For this reason we have not analyzed the majority of interferometry data. An example of one analyzed shot, however, is shown here in Figure 18. This shot was taken on suite 14-3, a SCFS target irradiated by a 300 Watt, 18.7 MHz, 3 $W/cm^2$ beam for about 3 seconds. As the figure shows, the density enhancement above ambient density can be significant, being as high as $10^{20}$ $atoms/cm^3$ in some places.

Examples of interferograms acquired under a variety of different conditions are shown in Figure 19. For irradiances higher then 3 $kW/cm^2$ a plume is seen each time. For some shots the plume is smooth and laminar indicating target material flow or heated air in front of the target. For other shots the diagnostic fringe pattern is convoluted, indicating complicated, though not turbulent, flow of gases in front of the target. At lower irradiances than 3 $kW/cm^2$ much less or no plume was seen.

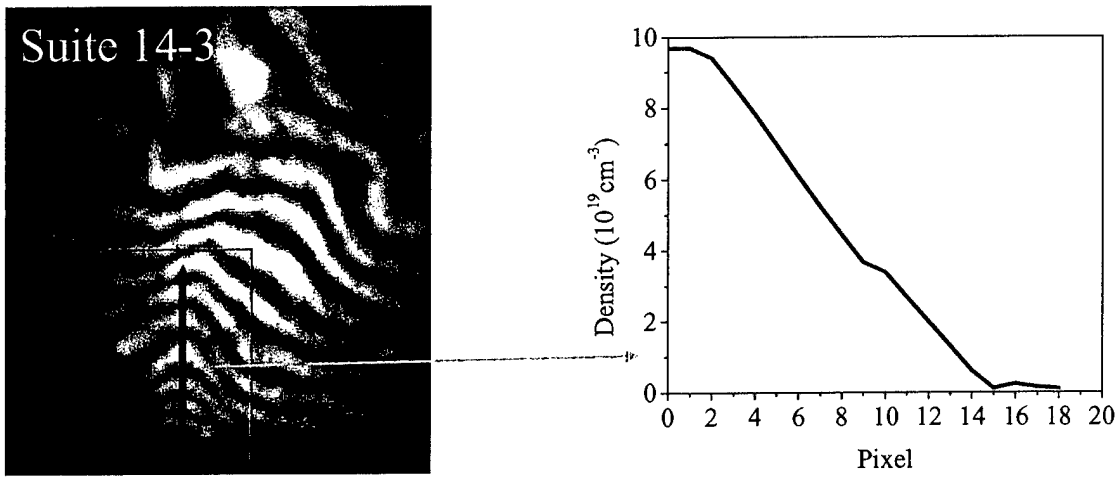


**Figure 18: Left: Interferograph taken at an unknown time during the exposure of Suite 14-3. The target is at the bottom of the picture with its normal pointing up. The FEL laser heats the target from the top producing the disturbance in the interferograph. Right: Density above ambient of gaseous material in front of the target along the red arrow in the figure on the left.**

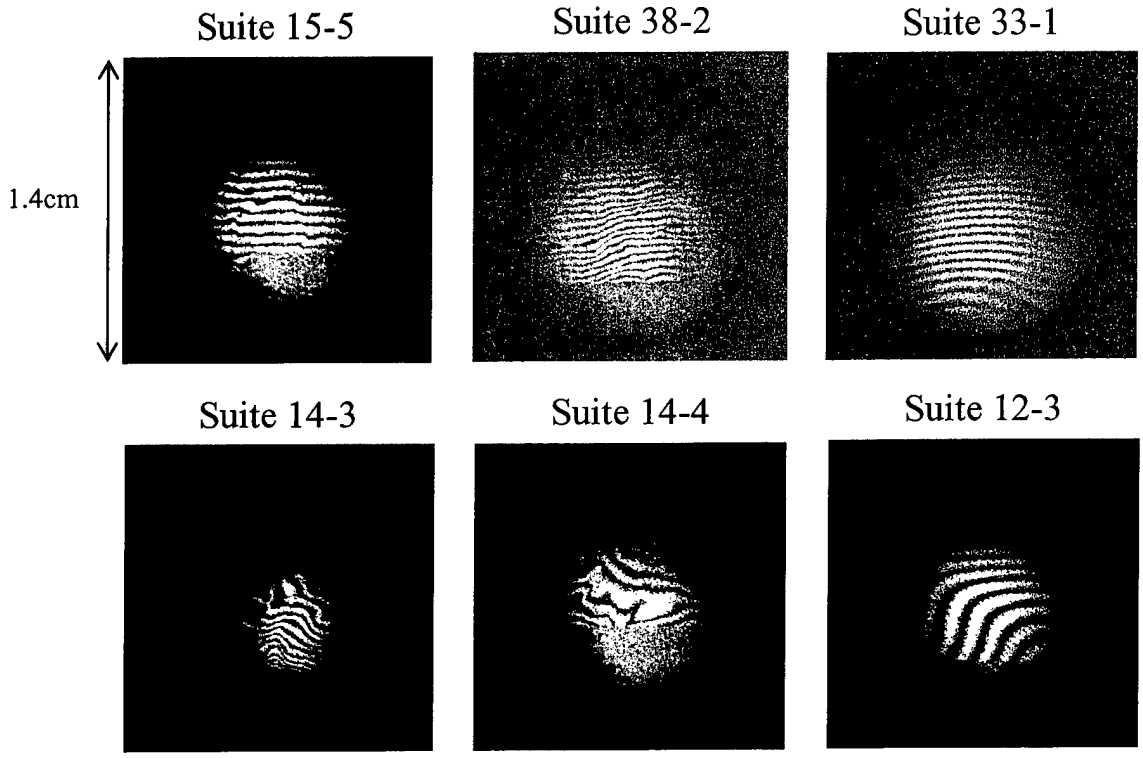


**Figure 19: Sample interferographs showing plumes in front of irradiated targets. In all cases the target is on the bottom of the interferograph with its normal pointing up and the FEL laser is incident from the top. The irradiation conditions are as follows: Suite 15-5; Target type 2, 1000W, 18.7MHz, 3KW/cm$^2$. Suite 38-2; Target type 3, 1000W, 37.4MHz, 3KW/cm$^2$. Suite 33-1; Target type 1, 300W, 18.7MHz, 3KW/cm$^2$. Suite 14-3; SCFS, 300W, 18.7MHz, 3KW/cw$^2$. Suite 14-4; Target type 2, 300W, 18.7MHz, 3KW/cm$^2$, Suite 12-3; Stainless steel, 300W, 18.7MHz, 10KW/cm$^2$.**

## Summary and Suggestions

Samples of various materials, such as stainless steel, painted and unpainted aluminum, fused silica, and fiberglass, were irradiated by a train of picosecond-duration pulses from a free-electron-laser at irradiances of 0.5 to 10 kW/cm$^2$. *In situ*, time and space resolved diagnostics that would measure details of the laser-target interaction were fielded on the experiment. In one diagnostic images of light emitted from the laser-irradiated heated side of the samples were optically split into four components. Each image component was passed through a different narrow band interference filter and then the filtered images were recorded by a CCD video camera. Appropriate software was used to convert the images into temperature profiles and movies of the temporal evolution of the temperature were produced. Heating and cooling of the samples, hole-burning, and flow of liquid matter, were observed. In fiberglass composite sample breakup of the fibers was recorded. A similar diagnostic placed to observe the rear side of the sample measured heating of the sample rear and details of the burn through. Light emission from the focal region was also coupled into a time-resolved spectrometer that recorded visible lines and continuum for the target surface. Black-body fits to the continuum were converted into movies of the samples' spatially integrated front-surface temperature. In addition, density of the vapor plume and heated air in front of the sample were measured with time resolved interferometry.

Surprisingly, the measurements showed that temperature profiles on the laser irradiated side of the target were flat-shaped even though the targets were irradiated by a Gaussian-like laser profile. This is probably due to the surface temperature becoming clamped at

the melting temperature of the sample and shows that uniform temperature results can be obtained even with non-uniform beams. Around the edges of some samples temperatures close to boiling temperatures of the materials were measured. At some laser powers most or the entire sample appeared to reach boiling temperatures. Temperature rise-times of the samples varied a lot depending on details of the experiment, such as laser powers, sample composition, exposure duration, and sample dimensions.

Temperature profiles of fiberglass composite samples exhibited a range of temperatures indicative of different processes occurring in different parts of the composite: Regions of resin cook-off, sublimation of carbonized char and the decomposition of the fiber cloth were measured. Flow of liquid material on the surfaces of fused silica samples was also observed. On samples irradiated at laser intensities of about $10kW/cm^2$ plumes of significant density were observed in front of the samples.

Q* measurements on metal and SCFS samples were much higher on this FEL than Q* measured on other lasers under similar irradiance conditions. The likely reason for this is the small spot sizes used in these experiments and the lack of strong airflow over the sample surface. These shortcomings will be corrected in future experiments when the FEL is upgraded to 10 kWatts and a well characterized air flow nozzle is constructed.

In all, the diagnostics functioned very well. In future experiments we suggest the following improvements:

- Provision for synchronization with individual FEL pulses

- Common timing for all diagnostics
- Simultaneous fielding of 4-frame diagnostic on the front and rear side of the target
- Greater temperature sensitivity of four frame and spectroscopy diagnostics
- Greater dynamic range for the four frame and spectroscopy diagnostics
- Two-color interferometry to measure dynamics of plumes having both neutral and ionized gas components
- A method to acquire more than one frame of interferometry per test
- Dedicated network links between diagnostics and control room
- Ability to remotely adjust filters and aperture diameters

It would also be valuable to field other space and time resolved diagnostics to measure absorption and reflectivity, temperature at locations other than the surface, and to install diagnostics to measure the presence and effects of shocks that should be generated at higher irradiances.

## Acknowledgments

The authors would like to thank, Major Franz Gayl (retired), Dr. Richard Gullickson, and Cmdr. Roger McGinnis for their support. We are also grateful to the staff at the Jefferson Laboratory whose professional and dedicated support made these experiments possible. This work was supported by the High Energy Laser Joint Technology Office (HEL-JTO).

## List of In-Situ Data

Below is a version of the shot matrix of all the high-energy-laser-lethality tests performed at JLAB during June 20 to 30, 2001 and September 17 to 28, 2001.[1] In the "slot" column we added in bold letters and highlighted in yellow the following symbols indicating the existence of good quality data:

- 4F - four frame camera space and time resolved temperature data on the front laser-irradiated side of the target
- 4Fb - four frame camera data on the back space and time resolved temperature data side of the target
- SP - Time resolved, spatially integrated temperature calculated from emission spectra
- PL - Plume interferometry data (not reduced to density)

When more then one diagnostics produced good results, these symbols are separated by slashes, ex. **(4F/SP/PL)**.

| ***June Shot Matrix* with Good In-Situ Diagnostic Data Indicated** | | | | | | | |
|---|---|---|---|---|---|---|---|
| **Suite** | **Slot 1** | **Slot 2** | **Slot 3** | **Slot 4** | **Slot 5** | **Slot 6** | **Run Parameters** |
| 1 | Plexiglas | Plexiglas | Plexiglas | Kentek | Kentek | Kentek | 300 W, 18.7 MHz, 1kW/cm$^2$ all 0.1sec |
| 2 | Plexiglas | Plexiglas | Plexiglas | Plexiglas | Plexiglas | Plexiglas | 300 W, 18.7 MHz, 3kW/cm$^2$ S1-S4 1sec, S5-S6 2sec |
| 3 | Plexiglas | Plexiglas | Plexiglas | Plexiglas | Plexiglas | Plexiglas | 300 W, 18.7 MHz, 10kW/cm$^2$ S1-S2 0.1sec, S3 1sec, S4 1sec, S5 0.5sec |
| 4 | 1" dia S.S. 0.0625 thk | 1" dia S.S. 0.0625 thk | 1" dia S.S. 0.0625 thk | Blank | Blank | Blank | 300 W, 18.7 MHz, 10kW/cm$^2$ various times to burnthrough |
| 5 | Blank | Blank | Blank | 1" dia S.S. 0.0625 thk | 1" dia S.S. 0.0625 thk | 1" dia S.S. 0.0625 thk | 300 W, 18.7 MHz, 3kW/cm$^2$ 20sec for all samples |
| 6 | 1" dia S.S. 0.0625 thk | 1" dia S.S. 0.0625 thk | 1" dia S.S. 0.0625 thk | Blank | Blank | Blank | 300 W, 18.7 MHz, 3kW/cm$^2$ 20sec for all samples |
| 7 | Blank | Blank | Blank | 1" dia S.S. 0.0625 thk | 1" dia S.S. 0.0625 thk | 1" dia S.S. 0.0625 thk | 300 W, 18.7 MHz, 10kW/cm$^2$ S4 30sec, S5 20sec, S6 20sec |
| 8 | 0.25" dia S.S. 0.0625 thk | 0.25" dia S.S. 0.0625 thk | 0.25" dia S.S. 0.0625 thk | 0.25" dia S.S. 0.0625 thk | 0.25" dia S.S. 0.0625 thk | 0.25" dia S.S. 0.0625 thk | 300 W, 18.7 MHz, 10kW/cm$^2$ all samples run to burnthrough |
| 9 | 1" dia Al. 0.0625 thk | 1" dia Al. 0.0625 thk | Blank | Blank | Blank | Blank | 300 W, 18.7 MHz, 10kW/cm$^2$ S1 20sec, S2, two shots @ 60sec |
| 10 | 1" dia S.S. 0.0625 thk | 1" dia S.S. 0.0625 thk | 1" dia S.S. 0.0625 thk | Blank | Blank | Blank | 300 W, 18.7 MHz, 1kW/cm$^2$, S1 10sec irrad., S2 15sec, S3 20 sec, S4 25 sec, S5 30 sec, S6 35 sec or to burn through |
| 11 | 1" dia S.S. 0.0625 thk | 1" dia S.S. 0.0625 thk **(PL)** | 1" dia S.S. 0.0625 thk **(PL)** | 1" dia S.S. 0.0625 thk | 1" dia S.S. 0.0625 thk | 1" dia S.S. 0.0625 thk | 300 W, 18.7 MHz, 3kW/cm$^2$, 5 sec irrad., S2 6 sec, S3 7 sec, S4 8 sec, S5 9 sec; S6 to burn through |
| 12 | 1" dia S.S. 0.0625 thk | 1" dia S.S. 0.0625 thk | 1" dia S.S. 0.0625 thk | 1" dia S.S. 0.0625 thk | 1" dia S.S. 0.0625 thk | 1" dia S.S. 0.0625 thk | 300 W, 18.7 MHz, 10kW/cm$^2$, 5 sec irrad., S2 6 sec, S3 7 sec, S4 8 sec, S5 9 sec; S6 to burn through |

| | | | | | | | |
|---|---|---|---|---|---|---|---|
| | **(PL)** | **(PL)** | **(PL)** | **(PL)** | | | |
| 13 | 1" dia SCFS **(PL)** | 1" dia SCFS **(PL)** | 1" dia SCFS **(PL)** | 1" dia target 2 **(PL)** | 1" dia target 2 **(PL)** | 1" dia target 2 **(PL)** | 300 W, 18.7 MHz, 1kW/cm$^2$, 8 sec irrad., or to burn through |
| 14 | 1" dia SCFS **(PL)** | 1" dia SCFS **(PL)** | 1" dia SCFS **(PL)** | 1" dia target 2 **(PL)** | 1" dia target 2 **(PL)** | 1" dia target 2 | 300 W, 18.7 MHz, 3kW/cm$^2$, 3 sec irrad., or to burn through |
| 15 | 1" dia SCFS **(PL)** | 1" dia SCFS **(PL)** | 1" dia SCFS **(PL)** | 1" dia target 2 **(PL)** | 1" dia target 2 **(PL)** | 1" dia target 2 | 300 W, 18.7 MHz, 10kW/cm$^2$, 3 sec irrad., or to burn through |
| 16 | 1" dia target 1 | 1" dia target 1 | 1" dia target 1 | 1" dia F2 | 1" dia F2 | 1" dia F2 | 300 W, 18.7 MHz, 1kW/cm$^2$, 8 sec irrad., or to burn through |
| 17 | 1" dia target 1 | 1" dia target 1 | 1" dia target 1 | 1" dia F2 | 1" dia F2 | 1" dia F2 | 300 W, 18.7 MHz, 3kW/cm$^2$, 8 sec irrad., or to burn through |
| 18 | 1" dia target 1 | 1" dia target 1 | 1" dia target 1 | 1" dia F2 | 1" dia F2 | 1" dia F2 | 300 W, 18.7 MHz, 10kW/cm$^2$, 8 sec irrad., or to burn through |
| 19 | 1" dia S.S. 0.125 thk | 1" dia S.S. 0.0625 thk | 1" dia S.S. 0.0625 thk | 1" dia S.S. 0.0625 thk | 1" dia S.S. 0.0625 thk | 1" dia S.S. 0.0625 thk | 300 W, 18.7 MHz, 1kW/cm$^2$, S1 10sec irrad., S2 15sec, S3 20 sec, S4 25 sec, S5 30 sec, S6 35 sec or to burn through |
| 20 | 1" dia S.S. 0.125 thk | 1" dia S.S. 0.0625 thk | 1" dia S.S. 0.0625 thk | 1" dia S.S. 0.0625 thk | 1" dia S.S. 0.0625 thk | 1" dia S.S. 0.0625 thk | 300 W, 18.7 MHz, 3kW/cm$^2$, S1 5 sec irrad., S2 10 sec, S3 15 sec, S4 20 sec, S5 25 sec; S30 to burn through |
| 21 | 1" dia S.S. 0.125 thk | 1" dia S.S. 0.0625 thk | 1" dia S.S. 0.0625 thk | 1" dia S.S. 0.0625 thk | 1" dia S.S. 0.0625 thk | 1" dia S.S. 0.0625 thk | 300 W, 18.7 MHz, 10kW/cm$^2$, S1 5 sec irrad., S2 10 sec, S3 15 sec, S4 20 sec, S5 25 sec; S6 30sec.. |
| 22 | 1" dia S.S. 0.0625 thk | 1" dia S.S. 0.0625 thk | 1" dia S.S. 0.0625 thk | 1" dia S.S. 0.0625 thk | 1" dia S.S. 0.0625 thk | 1" dia S.S. 0.0625 thk | 300 W, 74.85 MHz, 10kW/cm$^2$, 5 sec irrad., S2 10 sec, S3 15 sec, S4 20 sec, S5 25 sec; S6 30 to burn through |
| 23 | 1" dia S.S. 0.0625 thk **(4F/PL)** | " dia S.S. 0.0625 thk **(PL)** | 1" dia S.S. 0.0625 thk | " dia S.S. 0.0625 thk **(PL)** | " dia S.S. 0.0625 thk **(PL)** | 1" dia S.S. 0.0625 thk **(PL)** | 1000 W, 74.85 MHz, 10kW/cm$^2$, 5 sec irrad., S2 10 sec, S3 15 sec, S4 20 sec, S5 25 sec; S6 30 to burn through |

| | | | | | | | |
|---|---|---|---|---|---|---|---|
| 24 | 1" dia S.S. 0.0625 thk **(4F/PL)** | 1" dia S.S. 0.0625 thk **(4F/PL)** | 1" dia S.S. 0.0625 thk **(4F/PL)** | 1" dia S.S. 0.0625 thk **(4F/PL)** | 1" dia S.S. 0.0625 thk **(4F/PL)** | 1" dia S.S. 0.0625 thk **(PL)** | 1000 W, 74.85 MHz, 3kW/cm$^2$, 5 sec irrad., S2 10 sec, S3 15 sec, S4 20 sec, S5 25 sec; S6 30 or to burn through |
| 25 | 1" dia Pyroceram. 0.0625 thk **(4F/PL)** | 1" dia Pyroceram. 0.0625 thk **(PL)** | 1" dia Pyroceram. 0.0625 thk **(4F/PL)** | 1" dia Pyroceram. 0.0625 thk | 1" dia Pyroceram. 0.0625 thk | 1" dia Pyroceram. 5mm thk **(4F/PL)** | 1000 W, 74.85 MHz, 3kW/cm$^2$, ~1 sec irrad., S2 2 sec, S3 3 sec, S4 4 sec, S5 5 sec; S6 30 or to burn through |
| 26 | 1" dia Pyroceram. 5 mm thk **(4F/PL)** | 1" dia Pyroceram. 5 mm thk **(PL)** | 1" dia Pyroceram. 5 mm thk **(PL)** | 1" dia Pyroceram. 5 mm thk **(PL)** | 1" dia Pyroceram. 5 mm thk **(PL)** | 1" dia Pyroceram. 5mm thk **(4F/SP/PL)** | 1000 W, 74.85 MHz, 10kW/cm$^2$, ~2 sec irrad., S2 3 sec, S3 4 sec, S4 5 sec, S5 6 sec; S6 6 sec |
| 27 | 1" dia SCFS **(PL)** | 1" dia SCFS **(PL)** | 1" dia SCFS | 1" dia SCFS | 1" dia SCFS | 1" dia SCFS | 1000 W, 74.85 MHz, 3kW/cm$^2$, ~2 sec irrad., S2 3 sec, S3 4 sec, S4 5 sec, S5 6 sec; S6 6 sec |
| 28 | 1" dia SCFS **(4F/PL)** | 1" dia SCFS | 1" dia SCFS | 1" dia SCFS **(4F)** | 1" dia SCFS | 1" dia SCFS **(4F)** | 1000 W, 74.85 MHz, 10 kW/cm$^2$, ~2 sec irrad., S2 2 sec, S3 3 sec, S4 3 sec, S5 4 sec; S6 4 sec |
| 29 | 1" dia target 2 **(4F/SP)** | 1" dia target 2 **(PL)** | 1" dia target 2 **(PL)** | 1" dia F2 **(4F/PL)** | 1" dia F2 | 1" dia F2 **(4F/PL)** | 1000 W, 74.85 MHz, 10kW/cm$^2$, ~2 sec irrad., S2 2 sec, S3 2 sec, S4 4 sec, S5 4 sec; S6 4 sec |
| 30 | 1" dia target 1 **(PL)** | 1" dia target 1 **(PL)** | 1" dia target 1 **(PL)** | 1" dia target 3 **(PL)** | 1" dia target 3 **(PL)** | 1" dia target 3 **(SP/PL)** | 1000 W, 74.85 MHz, 10kW/cm$^2$, ~2 sec irrad., S2 2 sec, S3 2 sec, S4 2 sec, S5 2 sec; S6 2 sec (or to burn through) |
| 31 | 1" dia painted Al **(PL)** | 1" dia painted Al **(PL)** | 1" dia painted Al (flush) **(PL)** | 1" dia Al **(PL)** | 1" dia Al | 1" dia Al (flush) **(PL)** | 1000 W, 74.85 MHz, >1kW/cm$^2$, ~2 sec irrad., S2 2 sec, S3 2 sec, S4 2 sec, S5 2 sec; S6 2 sec. |
| 32 | 1" dia target 2 **(PL)** | 1" dia target 2 **(PL)** | 1" dia target 2 (flush) **(PL)** | 1" dia F2 **(PL)** | 1" dia F2 **(PL)** | 1" dia F2 (flush) **(PL)** | 1000 W, 74.85 MHz, 1kW/cm$^2$, ~8 sec irrad., S2 8 sec, S3 8 sec, S4 8 sec, S5 8 sec; S6 8 sec, or to burn through |

| | | | | | | | |
|---|---|---|---|---|---|---|---|
| 33 | 1" dia target 1 **(PL)** | 1" dia target 1 **(PL)** | 1" dia target 1 **(PL)** | 1" dia F2 **(PL)** | 1" dia F2 **(SP/PL)** | 1" dia F2 (flush) **(PL)** | 300 W, 18.7 MHz, 3 kW/cm$^2$, 1 ms, 60 Hz ~30 sec irrad., S2 30 sec, S3 30 sec, S4 30 sec, S5 30 sec; S6 to burn through |
| 34 | 1" dia SCFS **(PL)** | 1" dia SCFS **(PL)** | 1" dia SCFS **(PL)** | 1" dia SCFS **(PL)** | 1" dia SCFS **(PL)** | 1" dia SCFS (flush) **(PL)** | 300 W, 18.7 MHz, 3 kW/cm$^2$, 200 ms, 2 Hz ~30 sec irrad., S2 30 sec, S3 30 sec, S4 1 ms 60 Hz 30 sec, S5 30 sec; S6 60 sec., or to burn through |
| 35 | 1" dia Pyroceram 5 mm thk | 1" dia SCFS. | 1" dia F2 **(PL)** | 1" dia target2 | 1" dia target 1 | 1" dia target 3 | 1000 W, 37.4 MHz, 3 kW/cm$^2$, various irradiations |
| 36 | 1" dia Pyroceram 5 mm thk **(PL)** | 1" dia Pyroceram 5 mm thk **(PL)** | 1" dia Pyroceram 5 mm th**(PL)**k | 1" dia Pyroceram 5 mm thk | 1" dia Pyroceram 5 mm thk **(PL)** | 1" dia Pyroceram 5mm thk **(PL)** | 1000 W, 37.4 MHz, 3 kW/cm$^2$, 0.8 s, 2 Hz 4 sec irrad., S2 5 sec, S3 6 sec, S4 7 sec, S5 8 sec; S6 9sec., or to burn through |
| 37 | 1" dia F2 **(PL)** | 1" dia F2 **(PL)** | 1" dia F2 **(PL)** | 1" dia F2 | 1" dia F2 **(PL)** | 1" dia F2 **(PL)** | 1000 W, 37.4 MHz, 3 kW/cm$^2$, 30 ms, 15 Hz 12 sec irrad., S2 4 sec, S3 4 sec, S4 2 sec, S5 2 sec; S6 2sec., or to burn through |
| 38 | 1" dia target 3 | 1" dia target 3 **(SP/PL)** | 1" dia target 3 **(PL)** | 1" dia target 3 **(PL)** | 1" dia target 3 | 1" dia target 3 **(PL)** | 1000 W, 37.4 MHz, 3 kW/cm$^2$, 4 ms, 125 Hz 4 sec irrad., S2 1 sec, S3 1 sec, S4 2 sec, S5 2 sec; S6 2sec., or to burn through |
| 39 | 1" dia target 1 | 1" dia target 1 | 1" dia target 1 | 1" dia target 1 | 1" dia target 1 | 1" dia target 1 **(SP)** | 1000 W, 37.4 MHz, 3 kW/cm$^2$, 4 ms, 125 Hz 2 sec irrad., S2 2 sec, S3 4 sec, S4 4 sec, S5 4 sec; S6 4 sec., or to burn through |
| 40 | 1" dia target 2 **(PL)** | 1" dia target 2 **(PL)** | 1" dia target 2 **(PL)** | 1" dia target 2 **(PL)** | 1" dia target 2 **(PL)** | 1" dia target 2 **(PL)** | 1000 W, 37.4 MHz, 3 kW/cm$^2$, 30 ms, 15 Hz 6 sec irrad., S2 6 sec, S3 12 sec, S4 12 sec, S5 18 sec; S6 18sec., or to burn through |
| 41 | 1" dia SCFS | 1" dia SCFS | 1" dia SCFS | 1" dia SCFS | 1" dia SCFS | 1" dia SCFS | 1000 W, 37.4 MHz, 3 kW/cm$^2$, 1 s, 0.5 Hz 6 sec irrad., S2 6 sec, S3 12 sec, S4 12 sec, S5 18 sec; |

| | | | | | | | |
|---|---|---|---|---|---|---|---|
| | **(PL)** | **(PL)** | **(PL)** | **(PL)** | **(PL)** | (flush) **(PL)** **(PL)** | S6 18sec., or to burn through |

***September Shot Matrix*** with Good In-Situ Diagnostic Data Indicated

| Suite | Slot 1 | Slot 2 | Slot 3 | Slot 4 | Slot 5 | Slot 6 | Run Parameters |
|---|---|---|---|---|---|---|---|
| 42 | 1" dia Plexiglas | 1" dia Plexiglas | 1"dia Plexiglas | 1" dia Plexiglas | 1" dia Plexiglas | 1" dia Plexiglas | 300 W, 18.7 MHz, 1kW/cm$^2$, S1 2sec, S2 2sec, S3 2 sec, 300 W, 18.7MHz, 3 kW/cm$^2$ S4 2 sec, S5 2 sec, S6 2 sec |
| 43 | 1" dia Plexiglas | 1" dia Plexiglas | 1"dia Plexiglas | 1" dia Plexiglas | 1" dia Plexiglas | 1" dia Plexiglas | 300 W, 18.7 MHz, 10kW/cm$^2$, 2 sec irrad., S2 2 sec, S3 2 sec, 300 W, 74.85 MHz, 1kW/cm$^2$ S4 2 sec, S5 2 sec; S6 2 sec |
| 44 | 1" dia Plexiglas | 1" dia Plexiglas | 1"dia Plexiglas | 1" dia Plexiglas | 1" dia Plexiglas | 1" dia Plexiglas | 300 W, 74.85 MHz, 3kW/cm$^2$, 2 sec irrad., S2 2 sec, S3 2 sec 300 W, 74.85 MHz, 10kW/cm$^2$, S4 2 sec, S5 2 sec; S6 2 sec |
| 45 | 1" dia Plexiglas | 1" dia Plexiglas | 1"dia Plexiglas | 1" dia Plexiglas | 1" dia Plexiglas | 1" dia Plexiglas | 1kW, 74.85 MHz, 1kW/cm$^2$, 2 sec irrad., S2 2 sec, S3 2 sec, 3kW/cm$^2$ S4 2 sec, S5 2 sec; S6 2 sec |
| 46 | 1" dia Plexiglas | 1" dia Plexiglas | 1"dia Plexiglas | 1"dia Plexiglas | 1"dia Plexiglas | Blank | 1kW, 74.85 MHz, 10kW/cm$^2$, 1 sec irrad., S2 1sec, S3 1sec S4 1sec, S5 5sec |
| 47 | 1" dia S.S. 0.0625 thk **(SP)** | 1" dia S.S. 0.0625 thk **(4F)** | 1" dia S.S. 0.0625 thk **(4F/SP)** | 1" dia S.S. 0.0625 thk **(4F)** | 1" dia S.S. 0.0625 thk | 1" dia S.S. 0.0625 thk | 300 W, 18.7 MHz, 1kW/cm$^2$ S1–S4 25 sec, S5-S6 20sec |
| 48 | 1" dia S.S. 0.0625 thk **(SP)** | 1" dia S.S. 0.0625 thk **(SP)** | 1" dia S.S. 0.0625 thk **(4F)** | 1" dia S.S. 0.0625 thk **(4F/SP)** | 1" dia S.S. 0.0625 thk | 1" dia S.S. 0.0625 thk **(SP)** | 300 W, 18.7 MHz, 3kW/cm$^2$ S1-S6 15 sec |
| 49 | 1" dia S.S. 0.0625 thk **(4F)** | 1" dia S.S. 0.0625 thk | 1" dia S.S. 0.0625 thk **(4F)** | 1" dia S.S. 0.0625 thk **(4F)** | 1" dia S.S. 0.0625 thk | 1" dia S.S. 0.0625 thk **(SP)** | 300 W, 18.7 MHz, 10kW/cm$^2$ S1-S6 10 sec |

| | | | | | | | |
|---|---|---|---|---|---|---|---|
| 50 | 1" dia S.S. 0.0625 thk **(4F)** | 1" dia S.S. 0.0625 thk **(4F)** | 1" dia S.S. 0.0625 thk **(4F/SP)** | 1" dia S.S. 0.0625 thk | 1" dia S.S. 0.0625 thk | 1" dia S.S. 0.0625 thk | 300 W, 74.85 MHz, 1kW/cm$^2$ S1 10 sec, S2-S6 20 sec |
| 51 | 1" dia S.S. 0.0625 thk **(SP)** | 1" dia S.S. 0.0625 thk **(4F)** | 1" dia S.S. 0.0625 thk **(4F)** | 1" dia S.S. 0.0625 thk **(4F/SP)** | 1" dia S.S. 0.0625 thk **(SP)** | 1" dia S.S. 0.0625 thk **(SP)** | 300 W, 74.85 MHz, 10kW/cm$^2$, S1-S6 15sec |
| 52 | 1" dia S.S. 0.0625 thk **(4F/SP/PL)** | 1" dia S.S. 0.0625 thk **(4F/SP)** | 1" dia S.S. 0.0625 thk **(SP)** | 1" dia S.S. 0.0625 thk **(4F)** | 1" dia S.S. 0.0625 thk **(SP/PL)** | 1" dia S.S. 0.0625 thk **(PL)** | 300 W, 74.85 MHz,3kW/cm$^2$, S1-S6 15 sec |
| 53 | 1" dia Al 0.0625 thk **(PL)** | 1" 1" dia Al 0.0625 thk **(PL)** | 1" dia Al 0.0625 thk **(PL)** | 1" dia Al 0.0625 thk **(PL)** | 1" dia Al 0.0625 thk **(PL)** | 1" dia Al 0.0625 thk **(PL)** | 300 W, 74.85 MHz, 3kW/cm$^2$, S1-S6 15 sec |
| 54 | 1" dia Al 0.0625 thk **(PL)** | 1" dia Al 0.0625 thk **(PL)** | 1" dia Al 0.0625 thk | 1" dia Al 0.0625 thk **(PL)** | 1" dia Al 0.0625 thk **(PL)** | 1" dia Al 0.0625 thk | 300 W, 18.7 MHz, 3kW/cm$^2$, S1-S6 15 sec |
| 55 | 1" dia painted Al 0.0625 thk **(4F/PL)** | 1" dia painted Al 0.0625 thk **(4F/PL)** | 1" dia painted Al 0.0625 thk **(4F/PL)** | 1" dia painted Al 0.0625 thk **(PL)** | 1" dia painted Al 0.0625 thk **(PL)** | 1" dia painted Al 0.0625 thk **(PL)** | 300 W, 18.7 MHz, 3kW/cm$^2$, S1-S6 15 sec |
| 56 | 1" dia painted Al 0.0625 thk **(PL)** | 1" dia painted Al 0.0625 thk **(PL)** | 1" dia painted Al 0.0625 thk **(PL)** | 1" dia painted Al 0.0625 thk **(PL)** | 1" dia painted Al 0.0625 thk **(PL)** | 1" dia painted Al 0.0625 thk **(PL)** | 300 W, 74.85 MHz, 3kW/cm$^2$, S1-S6 15 sec |
| 57 | 0.25" dia Al 0.125 thk | 0.25" dia Al 0.125 thk **(PL)** | 0.25" dia Al 0.125 thk **(PL)** | 0.25" dia Al 0.125 thk **(PL)** | 0.25" dia Al 0.125 thk **(PL)** | 0.25" dia Al 0.125 thk **(SP/PL)** | 300 W, 74.85 MHz, 10kW/cm$^2$, S1 1sec, S2 10 sec, S3-S6 2 sec irrad |
| 54A | 1" dia Al 0.125 thk **(PL)** | 1" dia Al 0.125 thk **(PL)** | 1" dia Al 0.125 thk **(PL)** | 1" dia Al 0.125 thk **(PL)** | 1" dia Al 0.125 thk **(PL)** | 1" dia Al 0.125 thk **(PL)** | 300 W, 18.7 MHz, 3kW/cm$^2$, S1-S6 15 sec |
| 55A | 1" dia | 1" dia | 1" dia | 1" dia | 1" dia | 1" dia | 300 W, 18.7 MHz, 3kW/cm$^2$, S1-S2 15 sec S3-S4 |

| | | | | | | | |
|---|---|---|---|---|---|---|---|
| | painted Al 0.125 thk | painted Al 0.125 thk | painted Al 0.125 thk | painted Al 0.125 thk | painted Al 0.125 thk | painted Al 0.125 thk | 20 sec, S5-S6 30 sec |
| 58 | 0.25" dia SS 0.125 thk **(PL)** | 0.25" dia SS 0.125 thk **(SP/PL)** | 0.25" dia SS 0.125 thk **(PL)** | 0.25" dia SS 0.125 thk **(SP/PL)** | 0.25" dia SS 0.125 thk **(SP/PL)** | 0.25" dia SS 0.125 thk **(SP/PL)** | 300 W, 18.7 MHz, 10kW/cm$^2$, S1-S6 3 sec |
| 57A | 0.25" dia Al 0.125 thk | 0.25" dia Al 0.125 thk | 0.25" dia Al 0.125 thk | 0.25" dia Al 0.125 thk | 0.25" dia Al 0.125 thk | 0.25" dia Al 0.125 thk | 300 W, 18.7 MHz, 10kW/cm$^2$, S1-S6 3 sec |
| 53A | 1" dia Al 0.125 thk | 1" dia Al 0.125 thk | 1" dia Al 0.125 thk | 1" dia Al 0.125 thk | 1" dia Al 0.125 thk | 1" dia Al 0.125 thk | 300 W, 74.85 MHz, 3kW/cm$^2$, S1-S6 15 sec |
| 56A | 1" dia painted Al 0.125 thk | 1" dia painted Al 0.125 thk | 1" dia painted Al 0.125 thk | 1" dia painted Al 0.125 thk | 1" dia painted Al 0.125 thk | 1" dia painted Al 0.125 thk | 300 W, 74.85 MHz, 3kW/cm$^2$, S1-S6 30 sec |
| 59 | 0.25" dia SS 0.125 thk **(SP/PL)** | 0.25" dia SS 0.125 thk **(PL)** | 0.25" dia SS 0.125 thk **(SP/PL)** | 0.25" dia SS 0.125 thk **(SP/PL)** | 0.25" dia SS 0.125 thk **(SP/PL)** | 00.25" dia SS 0.125 thk **(SP/PL)** | 300 W, 74.85 MHz, 3kW/cm$^2$, S1-S6 3 sec |
| 60 | 0.25" dia Al 0.125 thk **(4Fb/SP)** | 0.25" dia Al 0.125 thk **(SP)** | 0.25" dia Al 0.125 thk **(4Fb/PL)** | 0.25" dia Al 0.125 thk **(4Fb/SP/PL)** | 0.25" dia Al 0.125 thk **(SP/PL)** | 0.25" dia Al 0.125 thk **(PL)** | 300 W, 74.85 MHz, 10kW/cm$^2$, S1-S6 3 sec |
| 61 | 1" dia Al 0.125 thk | 1" dia Al 0.125 thk **(PL)** | 1" dia Al 0.125 thk **(PL)** | 1" dia Al 0.125 thk **(PL)** | 1" dia Al 0.125 thk **(4F/SP/PL)** | 1" dia Al 0.125 thk **(SP)** | 600 W, 74.85 MHz, ~1 kW/cm$^2$, 10 sec irrad., S2 10 sec, S3 10 sec, S4 10 sec, S5-S6 10 sec; S6 10 sec |
| 62 | 1" dia Al 0.125 thk | 1" dia Al 0.125 thk | 1" dia Al 0.125 thk | 1" dia Al 0.125 thk | 1" dia Al 0.125 thk | 1" dia Al 0.125 thk | 600 W, 74.85 MHz, 3 kW/cm$^2$, S1-S6 20 sec |
| 63 | 1" dia Al 0.125 thk **(4F/LP)** | 1" dia Al 0.125 thk **(4F/SP)** | 1" dia Al 0.125 thk | 1" dia Al 0.125 thk **(PL)** | 1" dia Al 0.125 thk **(SP/LP)** | 1" dia Al 0.125 thk **(SP/LP)** | 600 W, 74.85 MHz, 10 kW/cm$^2$, S1-S6 20 sec |
| 64 | Target 2 | Target 2 | Target 2 | Target 2 | Target 2 | Target 2 | 600 W, 74.85 MHz, ~1 kW/cm$^2$, S1-S3 3 sec. |

| | | | | | | | |
|---|---|---|---|---|---|---|---|
| | | **(4F/PL)** | **(4F/PL)** | **(PL)** | **(PL)** | **(PL)** | ~1 kW/cm$^2$ S3-S6 4 sec. |
| 65 | Target 2 | Target 2 **(4F/PL)** | Target 2 **(4F/PL)** | Target 2 **(4F/PL)** | Target 2 **(PL)** | Target 2 **(4F/PL)** | 600 W, 74.85 MHz, ~1 kW/cm$^2$, S1-S3 6 sec. ~1 kW/cm$^2$ S4-S5 10 sec, S6 20 sec. |
| 66 | SCFS **(PL)** | SCFS **(4F/SP/PL)** | SCFS **(4F/PL)** | SCFS | SCFS **(PL)** | SCFS **(PL)** | 600 W, 74.85 MHz, 1 kW/cm$^2$, 10 sec irrad., S2 10 sec, S3 15 sec, S4 15 sec, S5 20 sec; S6 20 sec |
| 67 | Target 2 **(SP/PL)** | Target 2 **(4F/SP/PL)** | Target 2 **(4F/SP/PL)** | Target 2 **(PL)** | Target 2 **(SP/PL)** | Target 2 **(PL)** | 600 W, 74.85 MHz, 3 kW/cm$^2$, S1-S2 10 sec. S3-S4 8 sec 3 kW/cm$^2$ S5-S6 6 sec. |
| 68 | Target 2 | Target 2 | Target 2 | Target 2 | Target 2 | Target 2 | 600 W, 74.85 MHz, 3 kW/cm$^2$, S1-S2 5sec irrad., 10 kW/cm$^2$ S3-S4 4 sec, S5-S6 2 sec |
| 69 | 1" dia painted Al 0.125 thk | 1" dia painted Al 0.125 thk | 1" dia painted Al 0.125 thk | 1" dia painted Al 0.125 thk | 1" dia painted Al 0.125 thk | 1" dia painted Al 0.125 thk | 600 W, 74.85 MHz, 3 kW/cm$^2$, 15 sec irrad., S2 15 sec, S3 15 sec, S4 20 sec, S5 20 sec; S6 20 sec |
| 70 | 1" dia painted Al 0.125 thk | 1" dia painted Al 0.125 thk **(4F)** | 1" dia painted Al 0.125 thk **(4F)** | 1" dia painted Al 0.125 thk | 1" dia painted Al 0.125 thk | 1" dia painted Al 0.125 thk | 600 W, 74.85 MHz, ~1kW/cm$^2$, 10 sec irrad., S2 10 sec, S3 10 sec, S4 20 sec, S5 20 sec; S6 20 sec |
| 71 | SCFS | SCFS | SCFS **(4F)** | SCFS **(4F/SP/PL)** | SCFS **(PL)** | SCFS **(SP/PL)** | 600 W, 74.85 MHz, 10 kW/cm$^2$, S1-S3 10 sec, S4 - S6 20 sec |
| 72 | 1" dia painted Al 0.125 thk **(4F)** | 1" dia painted Al 0.125 thk **(4F)** | 1" dia painted Al 0.125 thk | 1" dia painted Al 0.125 thk **(4F)** | 1" dia painted Al 0.125 thk **(4F/PL)** | 1" dia painted Al 0.125 thk **(PL)** | 600 W, 74.85 MHz, 10 kW/cm$^2$, S1-S3 15 sec, S4-S6 12 sec |
| 73 | 1" dia S.S. 0.125 thk **(4Fb/SP/PL)** | 1" dia S.S. 0.125 thk **(4Fb/PL)** | 1" dia S.S. 0.125 thk **(4Fb/SP/PL)** | 1" dia S.S. 0.125 thk **(SP/PL)** | 1" dia S.S. 0.125 thk **(SP/PL)** | 1" dia S.S. 0.125 thk **(PL)** | 600 W, 74.85 MHz, 1 kW/cm$^2$, S1-S3 15 sec, S4 20 sec S5 40sec S6 20sec |
| 74 | 1" dia S.S. 0.125 thk **(4Fb/SP/PL** | 1" dia S.S. 0.125 thk **(4Fb/SP/PL** | 1" dia S.S. 0.125 thk **(4Fb/PL)** | 1" dia S.S. 0.125 thk **(SP/PL)** | 1" dia S.S. 0.125 thk **(SP/PL)** | 1" dia S.S. 0.125 thk **(PL)** | 600 W, 74.85 MHz, 3 kW/cm$^2$, 15 sec irrad., S2 15 sec, S3 15 sec, S4 25 sec, S5 25 sec; S6 25 sec |

| | ) | ) | | | | | |
|---|---|---|---|---|---|---|---|
| 75 | 1" dia S.S. 0.125 thk **(PL)** | 1" dia S.S. 0.125 thk **(PL)** | 1" dia S.S. 0.125 thk **(PL)** | 1" dia S.S. 0.125 thk **(PL)** | 1" dia S.S. 0.125 thk **(PL)** | 1" dia S.S. 0.125 thk **(PL)** | 300 W, 74.85 MHz, 1 kW/cm$^2$, S1-S3 15 sec, S4-S6 25 sec |
| 76 | 1" dia S.S. 0.125 thk **(4F/PL)** | 1" dia S.S. 0.125 thk **(4F/PL)** | 1" dia S.S. 0.125 thk **(PL)** | 1" dia S.S. 0.125 thk **(4F/PL)** | 1" dia S.S. 0.125 thk **(4F)** | 1" dia S.S. 0.125 thk **(4F)** | 300 W, 74.85 MHz, 3 kW/cm$^2$, S1-S3 15 sec, S4-S6 25 sec |
| 77 | 1" dia S.S. 0.125 thk | 1" dia S.S. 0.125 thk **(4Fb/PL)** | 1" dia S.S. 0.125 thk **(4Fb/PL)** | 1" dia S.S. 0.125 thk | 1" dia S.S. 0.125 thk | 1" dia S.S. 0.125 thk | 300 W, 74.85 MHz, 10 kW/cm$^2$, S1-S3 15 sec, S4-S6 25 sec |
| 78 | SCFS **(PL)** | SCFS | SCFS **(SP/PL)** | SCFS **(PL)** | SCFS **(PL)** | SCFS **(PL)** | 600 W, 74.85 MHz, 3 kW/cm$^2$, S1-S3 10 sec, S4 - S6 20 sec |
| 79 | 1" dia S.S. 0.125 thk **(SP)** | 1" dia S.S. 0.125 thk **(4Fb/PL)** | 1" dia S.S. 0.125 thk **(4Fb/PL)** | 1" dia S.S. 0.125 thk **(PL)** | 1" dia S.S. 0.125 thk **(PL)** | 1" dia S.S. 0.125 thk **(PL)** | 600 W, 74.85 MHz, 10 kW/cm$^2$, S1-S3 15 sec, S4&S6 25 sec S5 50 sec |
| 80 | 1" dia S.S. 0.125 thk **(4F)** | 1" dia S.S. 0.125 thk **(4F)** | 1" dia S.S. 0.125 thk **(4F/SP)** | 1" dia S.S. 0.125 thk **(4F)** | 1" dia S.S. 0.125 thk | 1" dia S.S. 0.125 thk | 300 W, 18.7 MHz, 1 kW/cm$^2$, S1 15 sec irrad., S2 15 sec, S3 15 sec, S4 25 sec, S5 25 sec; S6 25 sec |
| 81 | 1" dia S.S. 0.125 thk **(4F)** | 1" dia S.S. 0.125 thk **(4F)** | 1" dia S.S. 0.125 thk **(4F)** | 1" dia S.S. 0.125 thk **(4F/SP)** | 1" dia S.S. 0.125 thk **(SP)** | 1" dia S.S. 0.125 thk | 300 W, 18.7 MHz, 3 kW/cm$^2$, S1-S3 15 sec, S4-S6 25 sec |
| 82 | 1" dia S.S. 0.125 thk | 1" dia S.S. 0.125 thk **(4Fb)** | 1" dia S.S. 0.125 thk **(4Fb)** | 1" dia S.S. 0.125 thk | 1" dia S.S. 0.125 thk **(SP)** | 1" dia S.S. 0.125 thk | 300 W, 18.7 MHz, 10 kW/cm$^2$, S1-S3 15 sec, S4-S6 25 sec |
| 83 | 1" dia painted Al 0.125 thk | 1" dia painted Al 0.125 thk | 1" dia painted Al 0.125 thk | 1" dia painted Al 0.125 thk | 1" dia painted Al 0.125 thk | 1" dia painted Al 0.125 thk | 1kW, 74.85 MHz, 0.5 kW/cm$^2$, S1 15 sec, S2-S3 10 sec S4 –S5 9 sec, S6 10 sec |
| 84 | Steel #1 **(4F)** | | Steel #2 **(SP)** | | Steel #3 **(SP)** | | 650 W, 74.85 MHz, 0.5 kW/cm$^2$, Run to burnthrough |
| 85 | 16 ply | | 16 ply | | 16 ply | | 650 W, 74.85 MHz, 0.5 kW/cm$^2$, 30 sec or to 1000 |

| | | | | | | | |
|---|---|---|---|---|---|---|---|
| | graphite epoxy #1 | | graphite epoxy #2 **(SP)** | | graphite epoxy #3 | | °C |
| 86 | 32 ply graphite epoxy #1 | | 32 ply graphite epoxy #2 | | 32 ply graphite epoxy #3 | | 650 W, 74.85 MHz, 0.5 kW/cm$^2$, 30 sec or to 1000 °C |
| 87 | 32 ply graphite epoxy/steel #4 | | 32 ply graphite epoxy/steel #6 | | 16 ply graphite epoxy/steel #5 | | 650 W, 74.85 MHz, 0.5 kW/cm$^2$, 30 sec or to 1000 °C |
| 88 | 1" dia S.S. 0.125 thk **(4F/SP/PL)** | 1" dia S.S. 0.125 thk **(4F/SP/PL)** | 1" dia S.S. 0.125 thk **(SP/PL)** | 1" dia S.S. 0.125 thk **(4F/SP/PL)** | 1" dia S.S. 0.125 thk **(SP/PL)** | 1" dia S.S. 0.125 thk **(SP/PL)** | 650 W, 74.85 MHz, 0.5 kW/cm$^2$, S1-S3 15 sec, S4-S6 25 sec |
| 89 | SCFS **(PL)** | SCFS **(PL)** | SCFS **(PL)** | Target 2 **(PL)** | Target 2 **(PL)** | Target 2 **(4F/PL)** | 650 W, 74.85 MHz, 0.5 kW/cm$^2$, S1-S3 15 sec, S4 20 sec, S5 18 sec , S6 17 sec |
| 90 | Steel#4 **(4Fb/PL)** | Steel#5 **(4Fb/SP/PL)** | 16 ply graphite epoxy #7 **(PL)** | 16 ply graphite epoxy #8 **(4Fb/PL)** | 32 ply graphite epoxy #7 | 32 ply graphite epoxy #8 | 650 W, 74.85 MHz, 0.5 kW/cm$^2$, S1-S2 to burnthrough (~ 18 sec) S3-S4 60 sec S5-S6 120 sec |
| 91 | Target 2 | Target 2 | Target 2 | SCFS | SCFS | SCFS | 650 W, 74.85 MHz, 10 kW/cm$^2$, S1-S3 15 sec, S4-S5 25 sec S6 30 sec |
| 92 | 1" dia painted Al 0.125 thk | 1" dia painted Al 0.125 thk | 1" dia painted Al 0.125 thk | 1" dia Al 0.125 thk | 1" dia Al 0.125 thk | 1" dia Al 0.125 thk | 650 W, 74.85 MHz, 10 kW/cm$^2$, S1 15 sec, S2-S3 12 sec, S4-S5 25 sec, S6 33 sec |
| 93 | 1" dia S.S. 0.0625 thk **(4Fb/SP/PL)** | 1" dia S.S. 0.0625 thk **(4Fb/PL)** | 1" dia S.S. 0.0625 thk **(SP/PL)** | 1" dia S.S. 0.0625 thk **(4Fb/SP/PL)** | 1" dia S.S. 0.0625 thk **(4Fb/SP/PL)** | 1" dia S.S. 0.0625 thk **(4Fb/PL)** | 300 W, 74.85 MHz, 10kW/cm$^2$, S1-S6 15sec |
| 94 | Kentek | Kentek | Kentek | Kentek | Kentek | Kentek | S1 650 W S2-S6 300 W, 74.85 MHz, 10kW/cm$^2$, |

| | | | | | | | |
|---|---|---|---|---|---|---|---|
| | | | | | | | S1-S6 15sec |
| 95 | SCFS | Plexiglas | Plexiglas | Plexiglas | Plexiglas | Plexiglas | 650 W, 74.85 MHz, 10 kW/cm$^2$, S1-S3 15 sec, S4-S6 25 sec |
| 96 | Kentek | Kentek | Kentek | Kentek | Kentek | Kentek | 650 W 74.85 MHz, different z positions 2 sec |
| 97 | 4"x4"x1" Plexiglas | | | | | | 650 W 74.85 MHz, 21 sec |